

FOR REFERENCE

NOT TO BE TAKEN FROM THIS ROOM

FRACTURE CHARACTERIZATION OF GRAY CAST IRON

by

OSMAN KURDAŞ

B.S. in M.E., Boğaziçi University, 1982

Submitted to the Institute for Graduate Studies in
Science and Engineering in partial fulfillment of the
requirements for the degree of

Master of Science

in

Mechanical Engineering

Bogazici University Library



39001100316010

14

Boğaziçi University

1983

ACKNOWLEDMENT

I would like to express my feelings of sincere gratitude to my thesis supervisor, Associate Proffesor Öktem Vardar for his invaluble guidance and friendly cooperation in the absence of which, the present work would not be possible at all.

Osman Kurdaş

December, 1983

ABSTRACT

The aim of this study is to investigate various fracture properties of gray cast iron and thus to gain an insight of its behaviour and reliability under conditions where there is a risk of brittle fracture or fatigue failure. Various K_{1c} fatigue, bending, K_{1sc} and tension tests are performed using the appropriate compact tension, three point bend and tensile specimens. Obtained results are resumed and interpreted besides pin pointing the consequences of the thesis.

ÖZET

Bu çalışmanın gayesi gri dökme demirin (kır döküm) genel kırılma özelliklerini saptamak, böylece bu malzemenin gevrek kırılma yahut yorulma tehlikesi olabilecek durumlardaki davranış biçimi ve güvenelirliği hakkında fikir sahibi olmaktır.

Uygun, ufak çekme, üç noktada eğme, K_{1gkk} ve çekme deneyleri yapılmıştır. Elde edilen sonuçlar özetlenmiş, yorumlanmış ve bu konuda yapılabilecek başka çalışmalar için bazı düşüncelere yer verilmiştir.

TABLE OF CONTENTS

	<u>PAGE</u>
ACKNOWLEDMENT	iii
ABSTRACT	iv
ÖZET	v
LIST OF FIGURES	viii
CHAPTER I INTRODUCTION	1
CHAPTER II LINEAR ELASTIC FRACTURE MECHANICS	3
1-Stress analysis of cracks	3
2- K_{Ic} test method	4
CHAPTER III STRESS CORROSION CRACKING	8
CHAPTER IV FATIGUE CRACK PROPAGATION	10
CHAPTER V YIELDING FRACTURE MECHANICS	12
1-J Integral	12
2-Evaluation of J_{Ic}	14
CHAPTER VI 1-Tension tests	15
a-Experimental setup and specimen	15
b-Experimental results	16
c-Analysis of results	17
2- Bending tests	19
a-Experimental setup and specimen	19
b-Experimental results	19
c-Analysis of results	20
3-Microscopic Examinations	22
4-Hardness tests	25
a-Apparatus and specimen	25
b-Experimental results	25

	<u>PAGE</u>
5-K _{1c} tests	26
a-Experimental setup and specimen	26
b-Experimental results	29
c-Analysis of results	29
6-K _{1SCC} tests	32
a-Experimental setup and specimen	32
b-Experimental results	33
c-Analysis of results	34
7-Fatigue tests	36
a-Experimental setup and specimen	36
b-Experimental results	36
c-Analysis of results	36
8-J ₁ tests	42
a-Experimental setup and specimen	42
b-Experimental results	42
CHAPTER VII CONCLUSIONS	46
APPENDIX A	48
APPENDIX B	52
APPENDIX C	57
APPENDIX D	67

LIST OF FIGURES

<u>FIGURE No</u>		<u>PAGE</u>
2.1.1	Basic modes of crack surface displacements	3
2.2.1	Effect of thickness on K_{1c} behaviour	5
2.2.2	ASTM compact tension specimen	5
2.2.3	Obtaining P_q from load vs. displacement plot	6
3.1	Behaviour in pre-cracked stress corrosion tests	8
4.1	Crack growth rate dependence on ΔK	10
5.1.1	Arbitrary contour around crack tip	13
5.1.2	Interpretation of J integral	13
6.1.2	Machining orientation of various specimens in CT specimen	16
6.1.3	Load vs. displacement behaviour of Specimen 13	18
6.2.1	TPB specimen used for bending tests	19
6.2.2	Bending test load vs. displacement behaviour	21
6.3.1	Microstructural view of Specimen 4	22
6.3.2	Microstructural view of Specimen 10	23
6.3.3	Microstructural view of Specimen 14	23
6.3.4	Microstructural view of Specimen 25	24
6.5.1	Steel clamps used for coupling the CTS to MTS fatigue machine	26
6.5.2	CTS for K_{1c} test	28
6.5.3	K_{1c} testing setup	28
6.5.4	Load vs. displacement plot of Specimen 10 obtained during K_{1c} test	31

<u>FIGURE No</u>		<u>PAGE</u>
6.6.1	TPB specimen geometry for K_{Isc} test	32
6.6.2	Schematic drawing of K_{Isc} testing apparatus	33
6.6.3	Initial K_{Ic} % vs.log time plot obtained from K_{Isc} test	35
6.7.1(a)	da/dN vs. ΔK behaviour of Specimens 5 and 6	37
6.7.1(c)	Combined da/dN behaviour of Specimens 5,6,7 and 18	39
6.8.1	Load vs. displacement plot obtained from J_1 test	43
6.6.2	J vs. Δa plot of Specimens 16,19 and 24	44
7.1	Fatigue behaviour of Specimen 5	63
7.2	Fatigue behaviour of Specimen 6	64
7.3	Fatigue behaviour of Specimen 7	65
7.4	Fatigue behaviour of Specimen 18	66

CHAPTER I

INTRODUCTION

It is a well known fact that brittle materials are always easily accesible and more abundant than ductile materials. However the unreliable behaviour posed by these kind of materials, under various kinds of static or dynamic tensile loadings, restricted their use, mainly into situations where there are only compressive loadings. Two or there decades ago engineers were simply avoiding the use of brittle materials under conditions where there is a tensile loading, but later getting more acquainted with the recent developments in fracture mechanics provided for them a means of designing against fracture in engineering structures, in a more quantitative manner than is possible using traditional toughness testing techniques. As a matter of fact this suggested a reconsideration of trustworthiness of brittle materials.

Among all metallic brittle materials cast iron is of special interest. The general term "cast iron" includes gray iron, pig iron white iron, chilled malleable and nodular iron. This article only deals with gray cast irons that are alloys of carbon and silicon in which more carbon is present than can be retained in solid solution in austenite at the eutectic temperature. The carbon in excess of austenite solubility in iron, precipitates as graphite flakes in the metal matrix. This material offers some unique properties such as extremely low costs, high damping capacity, wear resistance, good castability and machinability.

In spite of these refined qualities gray iron is not

considered as an alternative in applications where there is a possibility of brittle fracture and consequently no serious perseverance has been spent for determining the fracture properties of it. This study has been devoted for investigating various fracture properties of gray cast iron and the motivation behind it, was not only academic concern but also it was hoped to reveal out its behaviour, under tensile loading, thus obtaining some tangible results which may encourage the engineers to approach it in a less prejudiced manner.

Macroscopic fracture mechanics is a broad subject and both linear and ductile fracture mechanics offers various tests such as K_{1c} , J_{1c} , fatigue, drop weight, dynamic tear, K_{1sc} and so on. For this study K_{1c} , K_{1sc} and various fatigue tests were performed besides tensile, bending and hardness tests. Also some microscopic study has been made within the bounds of the possibilities offered by the metallurgical laboratory and some specimens are polished etched and their photographs are taken.

This article contains all the obtained results as well as their interpretations.

CHAPTER II

LINEAR ELASTIC FRACTURE MECHANICS

1- Stress analysis of cracks

The stress fields surrounding a crack tip can be divided into three major modes of loading that involve different crack surface displacements as shown in figure 2.1.1.

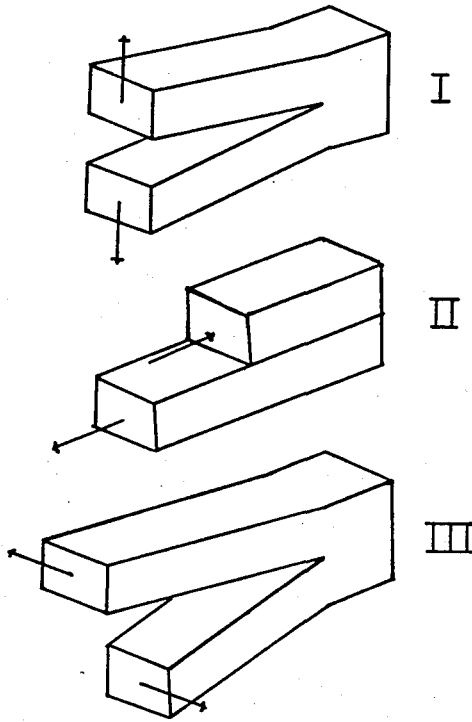


FIGURE 2.1.1-Basic modes of crack surface displacements

Mode I loading is encountered in the overwhelming majority of actual engineering situations involving cracked components. The crack tip stress expressions developed by Westergaard (see Appendix A-1) have an important feature such that the stress distribution around any crack depends only on the parameters r and θ . The difference between the individual cracked components lies in the magnitude of a parameter K defined as the "stress inten-

sity factor". Stress intensity factors (K_I , K_{II} or K_{III} depending on the loading mode) are a function of load, geometry and crack size. Evidently actual structural materials have some certain limiting characteristics such as S_y (yield strength) and as a matter of fact there is also a limiting value of stress intensity factor named "fracture toughness" (K_{IC}) at which unstable crack growth occurs. Fracture toughness is essentially the first move in every fracture test and considerable effort has been spent for developing a standardized procedure for its experimental determination. (8,9,6)

2- K_{IC} test method

Early in the development of the K_{IC} test methods it was established that, elastic fracture mechanics was the best analysis by which the resistance of materials to unstable crack growth could be described. Thus the early work of the ASTM committee was directed toward work on the elastic fracture problem. A rather interesting fact discovered by the committee was that, K_{IC} was dependent to specimen thickness up to a certain level above which it assumes a rather constant value (see figure 2.2.1).

That is, if conditions of plane strain can be fulfilled for a given specimen then it is possible to find the minimum value of K_{IC} which is a material constant. Taking this fact into account ASTM published a testing procedure (E-399-74) which then became a standard. First of all rather strict specimen dimensions were imposed in order to achieve plane strain behaviour (see figure 2.2.2)

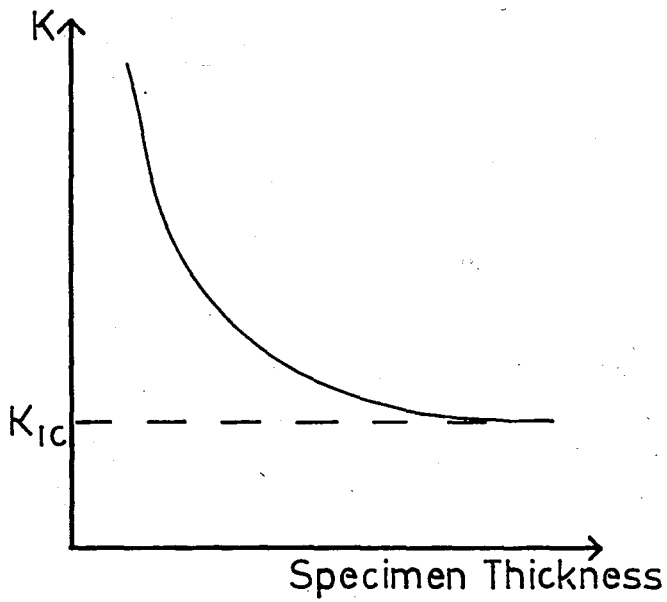
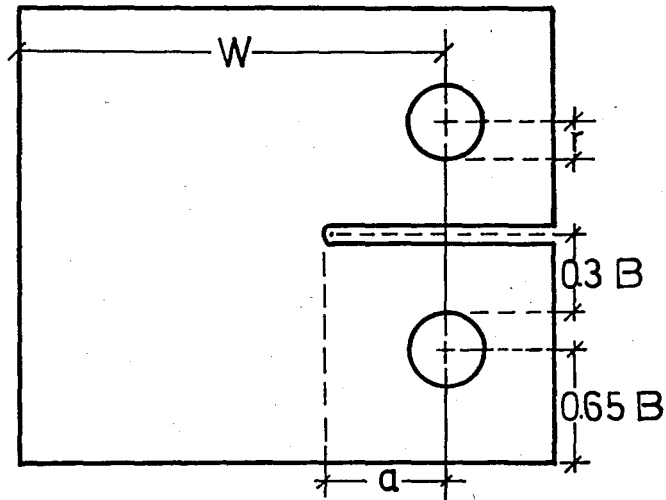


FIGURE 2.2.1-Effect of thickness on K_{IC} behaviour



B = thickness
 $W = 2 B$
 $a = B$
 $r = 0.25 B$

FIGURE 2.2.2-ASTM compact tension specimen (CTS)

The criteria for plane strain behaviour which are the results of some experimental study are as below:

$$\begin{aligned} a &\geq 2.5(K_{Ic}/S_y) \\ B &\geq 2.5(K_{Ic}/S_y) \\ W &\geq 5.0(K_{Ic}/S_y) \end{aligned} \quad (1)$$

Since K_{Ic} increases with notch root radius (4) a real sharp crack with zero root radius is essential and this can be obtained by fatigue pre-cracking the specimen before the test.

Experimental procedure:

- a-Fatigue pre-crack the specimen to obtain sharp crack.
- b-Load the specimen monotonically until fracture and simultaneously record load vs. front face displacement.
- c-Draw 5% secant line corresponding to 2% change in crack length.
- d-Obtain P_q from the graph (see figure 2.2.3). Check whether $(P_{max}/P_q) < 1.1$. If this criteria is not satisfied then the test is not valid.

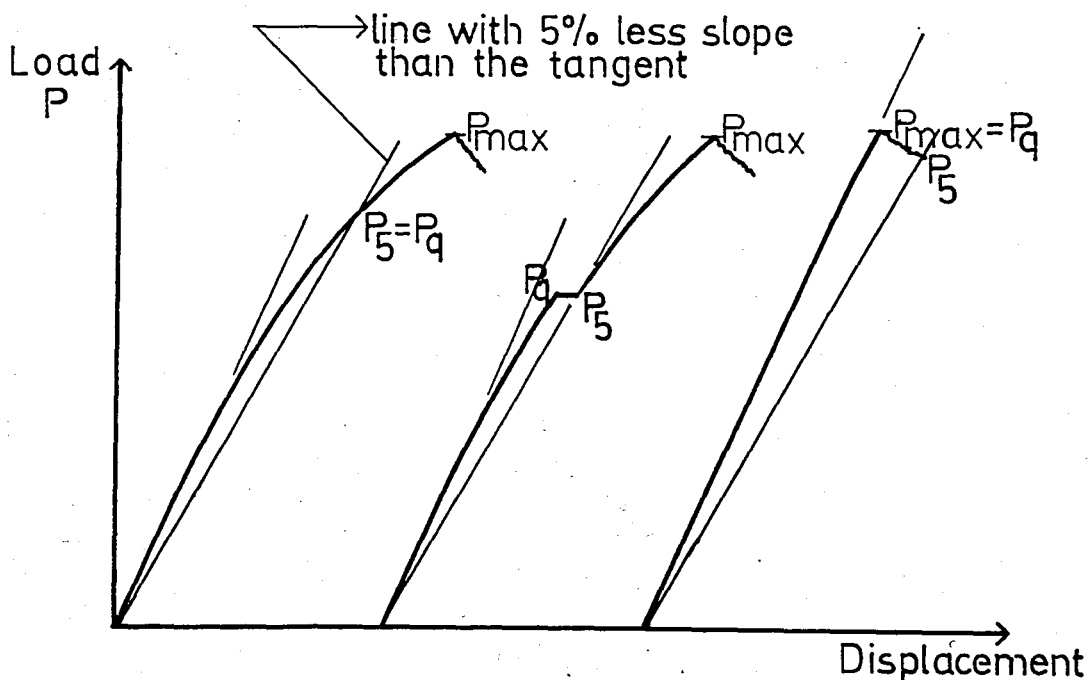


FIGURE 2.2.3-Obtaining P_q from load vs. displacement plot(8)

e-Use the appropriate K_1 expression (see Appendix A-2) to calculate K_q .

f- Check for validity of plane strain assumption by using equation (1). If the obtained K_q satisfies the three criteria then

$K_q = K_{1c}$, if not, choose a thicker specimen and repeat the test (4,6,8)

CHAPTER III

STRESS CORROSION CRACKING

Although one can usually be confident about his design based upon K_{Ic} , a frequently observed fact is that some engineering structures fail even at low stress intensity values, when they are exposed to some corrosive environment. Various investigations proved that in such cases crack propagation is stimulated by the simultaneous action of corrodent and stress. Numerous microscopic explanations were proposed in order to clarify the real mechanism of stress corrosion crack growth but there are still points that are debatable. Some specimens tend to last indefinitely in a corrodent at a sufficiently low value of K_I which is termed K_{Isc} and under these circumstances resistance to stress corrosion failure can be guaranteed by working with K_I values lower than K_{Isc} (see figure 3.1).

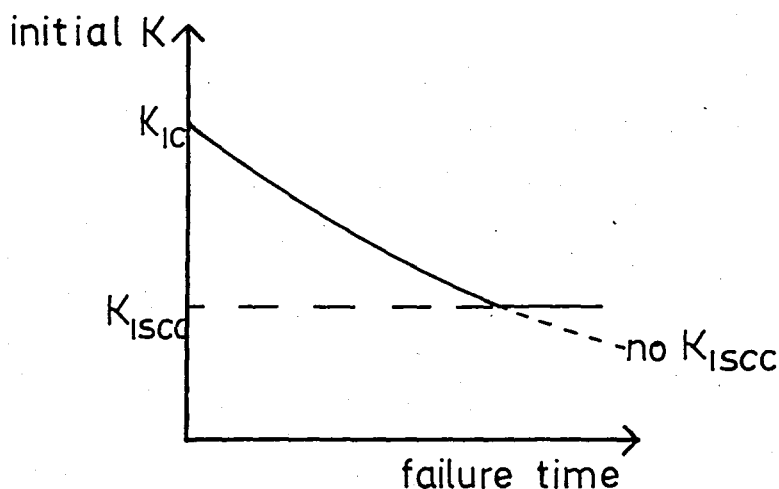


FIGURE 3.1-Behaviour in pre-cracked stress corrosion test (8)

K_{Isc} value is essentially both stress and environment dependent and an alloy may have a definite K_{Isc} or not depending on the kind of environment it is exposed to (1).

Classical stress corrosion tests are performed by stressing the specimens with static weights that produce bending moments and simultaneously exposing to the corrosive environment. Testing variables are usually the type of environment (chemical nature PH, temperature) and applied K level. Generally some creep is observed before final failure and this creep behaviour besides failure time, form the usual recorded data of the test. Usually there is no appreciable crack growth before the incubation period after which crack propagation becomes significant causing the applied K value to increase with time until final failure when $K=K_c$.

It is a well acquainted fact that as the crack tip radius increases, the load required for final failure also increases accordingly

(6). Similarly for stress corrosion tests crack tip radius plays an important role because, for a given loading amount, the magnitude of initial K generated at the crack tip is significantly smaller than that of a crack with a sharp notch thus, testing times tend increase drastically. Consequently it is usual practise to notch the specimens before the test by means of machining or fatigue pre-cracking (excluding the experiments which are performed without a notch on purpose).

Environmental assisted cracking is a relatively new subject and it still requires some further study for the clarification of the debatable points.

CHAPTER IV

FATIGUE CRACK PROPAGATION

Even if the working stress of a specimen has been assessed at a safe value there can still be catastrophic failures, owing to small defects that grow to critical lengths during operation by a "subcritical crack growth mechanism" such as fatigue. To provide a basis for fracture mechanics approach to fatigue crack propagation numerous experimental observations were made. A simple relationship of the form

$$da/dn = c \Delta K^m \quad (2)$$

was introduced by Paris (4). He observed that, at low values of crack extension crack propagation rate with respect to number of cycles (da/dn) increases rather rapidly which then settles down until a specific crack length after which the slope steepens again (see figure 4.1).

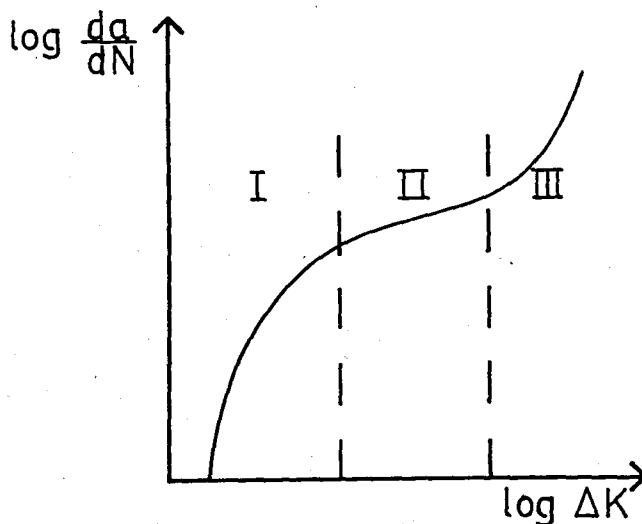


FIGURE 4.1-Crack growth rate dependence on ΔK (4,8)

Usually region II can be well represented by m values around 3-4 and it is this region that is thought to be worth considering generally, because in regions I and III crack propagation rates are somewhat inconsistent and a considerable portion of the total specimen life is spent in region II. An important thing to mention here is that, below a certain K value (depending on the kind of material) fatigue cracks do not propagate at all and the structure will have infinite life in terms of fatigue failure. This value of K is termed "threshold value" and ideally it is best to work below this value.

Many factors affect crack propagation rate, namely, mean value of stress, specimen thickness, specimen ductility, frequency of loading, inclusions in the material matrix and previous loading history of the specimen (3,9). A case in which previous loading history affects crack propagation rate to a considerable extent is the case of a single overload applied to a constant amplitude cycle which decreases the propagation rate over subsequent cycles. This effect may form as a consequence of several factors such as residual compressive stress that forms after overload, crack tip blunting during overload or from the crack closure mechanism (the closing of the crack faces even under tensile stress because of the residual stresses formed by the plastically deformed regions behind the crack tip). (4)

Fatigue crack propagation is a broad subject and there are still some debatable points including the micromechanisms of crack initiation and propagation.

CHAPTER V

YIELDING FRACTURE MECHANICS

1- J Integral

It was mentioned earlier that to obtain valid results for K_{1c} tests, plane strain conditions must be met which imposes the use of extremely large test specimens that may not represent the behaviour of actual sections used in service. Consequently some new parameters have been proposed to obtain tangible results with small specimens even under conditions of yield. Strain energy release rate called "J Integral" was proposed by Rice in 1968 and from then on it has been under focus of attention. J integral is defined as follows:

$$J = \int_{\Gamma} \left(W dy - t_i \frac{\partial u_i}{\partial x} ds \right) \quad (3)$$

Where t : traction vector

u : displacement vector

W : strain energy density

Γ : arbitrary contour around crack tip

J is a path independent line integral which means the shape and size of the boundary is arbitrary (see figure 5.1.1)

An appealing feature of J integral is that if Γ is taken as a circle of radius r , in an infinite body r can be allowed to tend to infinity so that the below relation holds:

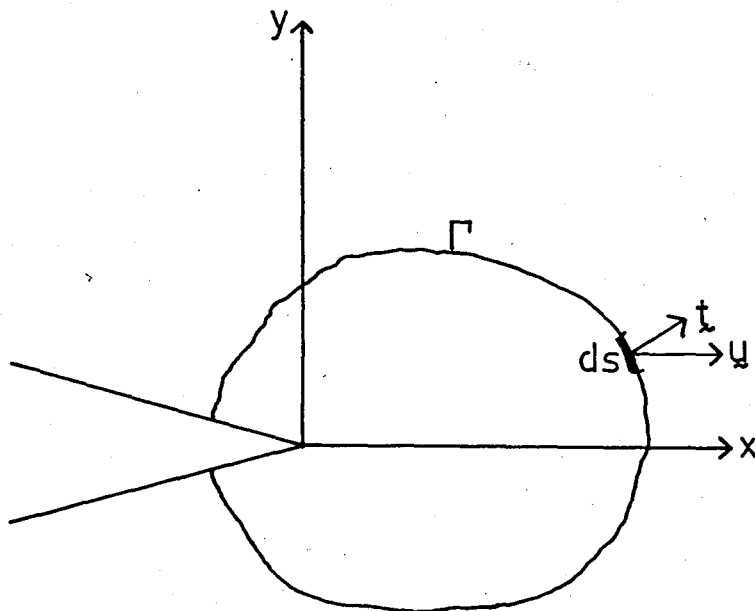
$$J = K^2 / E(1 - \nu^2) \quad (4)$$

From a physical viewpoint J may be interpreted as the potential energy difference between two identically loaded bodies having

neighbouring crack sizes or

$$J = -\frac{1}{B} \frac{\partial U}{\partial a} \quad (5)$$

Above definition is shown schematically in figure 5.1.2 .



t = traction vector
 u = displacement vector

FIGURE 5.1.1-Arbitrary contour around crack tip (4)

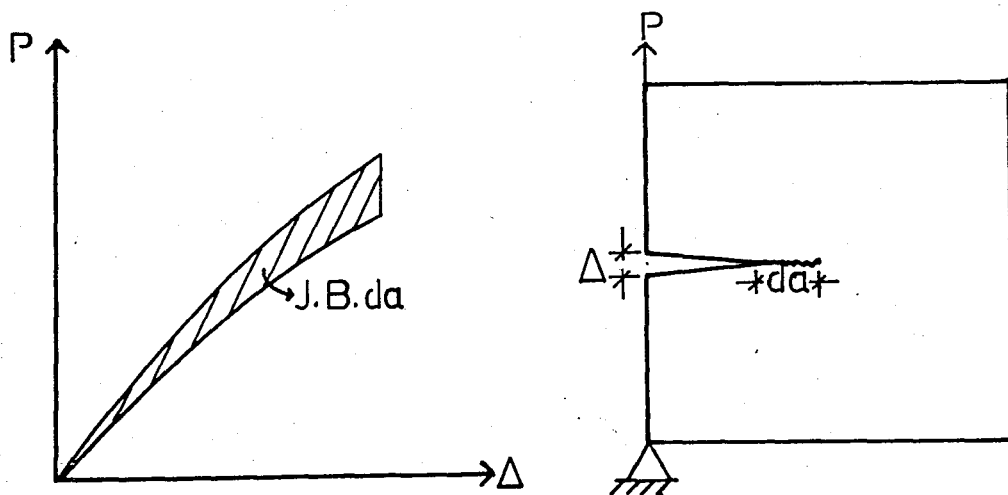


FIGURE 5.1.2-Interpretation of J integral (8)

J integral has some interesting advantages such as:

- a-J can be used to characterize the onset of crack extension in ductile materials. i.e. by determining J_{1c} in a small specimen large scale yielding test, the fracture toughness can be computed using equation (4). As a matter of fact large specimen sizes dictated by K_{1c} procedure can be eliminated (4,8,14).
- b-Under restricted circumstances toughness and stability of the extending crack can be analysed by using J_R resistance curve (14)
- c-Creep crack growth at elevated temperatures can be interpreted to some extent (14).

Concisely, J integral is a method that can be used to characterize the stress strain field at the tip of the crack.

2- Evaluation of J_{1c}

Various methods have been proposed to determine J_{1c} many of them still being tentative. Usually change of compliance with changing crack length is used for determining the crack advance which later is related to J_{1c} . In the recent years single specimen techniques became more popular due to their simplicity of application. A tentative test procedure using single specimen is placed in Appendix A-4.

CHAPTER VI

EXPERIMENTAL WORK

1- TENSION TESTS

a- Experimental setup and specimen preparation

For the simple tension tests MTS fatigue testing machine is used. It is suggested that as cast tension specimens must be casted as thick as the governing dimension of the actual structure to get rid of the differences due to thickness variation (such as cooling rate) (12). Unfortunately for the case in hand this application leads to 40 mm thick specimens which is quite impractical (too much machining work is required to obtain proper specimens). Therefore, for this study specimens are machined out from compact tension specimens that are used for the fracture tests. Specimen dimensions are chosen according to TS-138 J (see figure 6.1.1).

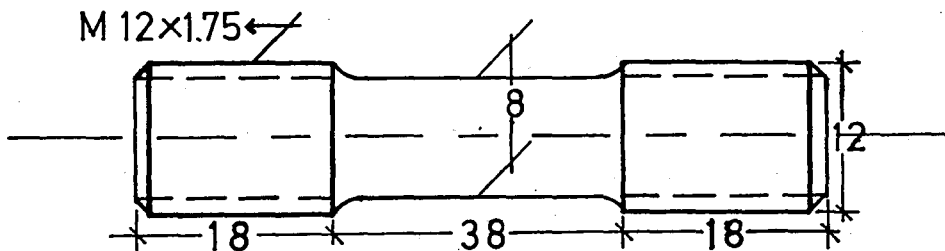


FIGURE 6.1.1- TS-138 J-8b type tensile specimen (in mm)

Orientation of the tensile specimens in CT specimens are as shown in figure 6.1.2 .It is assumed that changing this orientation will not affect the results significantly.

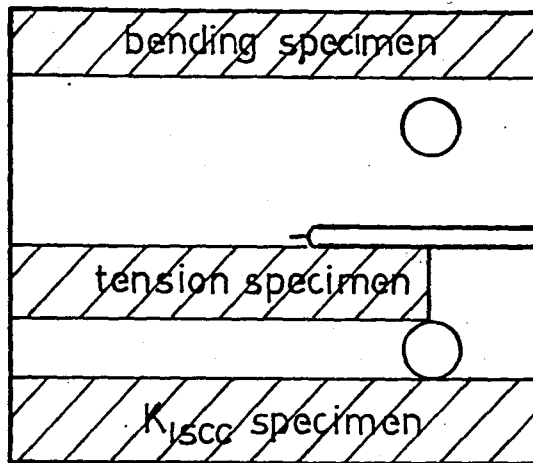


FIGURE 6.1.2-Machining orientation of various specimens in the compact tension specimen.

b- EXPERIMENTAL RESULTS

All together six tests were performed by monotonically loading the specimens until failure while recording the actuator piston displacement vs. load with a X-Y recorder. Below are the results of the tests:

SPECIMEN No	P_{yield} (kg)	P_{max} (kg)	$S_y^{(1)}$ (kg/mm ²)	S_{ut} (kg/mm ²)
101	353	420	7.5	9.0
010	405	440	8.0	9.0
133	705	830	14.0	16.0
313	660	690	13.0	13.5
144	435	520	9.0	10.0
114	525	600	10.5	12.0

(1):Yield load is found by 0.2 % strain offset technique

Apart from the tensile tests one single compression test is

performed with specimen 141 and a compressive strength of 37 kg/mm^2 is obtained, however due to the eccentricity of loading during compression this value is most probably lower than the true compressive strength. During the tests loading rate are kept constant (approximately 500 kg/minute).

c- ANALYSIS and DISCUSSION OF RESULTS

Obtained S_y and S_{ut} values are obviously scattered so it may be wise to calculate the mean of these two properties:

$$\bar{S}_y = 11 \text{ kg/mm}^2 \quad \bar{S}_{ut} = 12 \text{ kg/mm}^2$$

Above values are slightly lower than that of ASTM class 20 iron but one must bear in mind that in a tension test, even a slight eccentricity of loading may decrease the obtained values considerably. Nevertheless it is evident that the gray iron used for this study is of quite low strength. Load vs. displacement diagrams indicate a general nonlinear behaviour and as a matter of fact failures occurred abruptly giving no signs of necking above the yield strength (see figure 6.1.3).

The compact tension specimens used for obtaining tensile specimens were of different thicknesses (i.e: specimens 101 and 010 are from 20mm thick specimens while specimens 144 and 114 are from 40mm specimens) and this was done on purpose to measure the thickness effect on strength, however the results indicated that thickness variations does not affect the strength values appreciably (5,12).

It is difficult to obtain E (elastic modulus) by simply drawing a tangent and using hook's law because of the highly nonlinear load displacement plot (see figure 6.1.3).

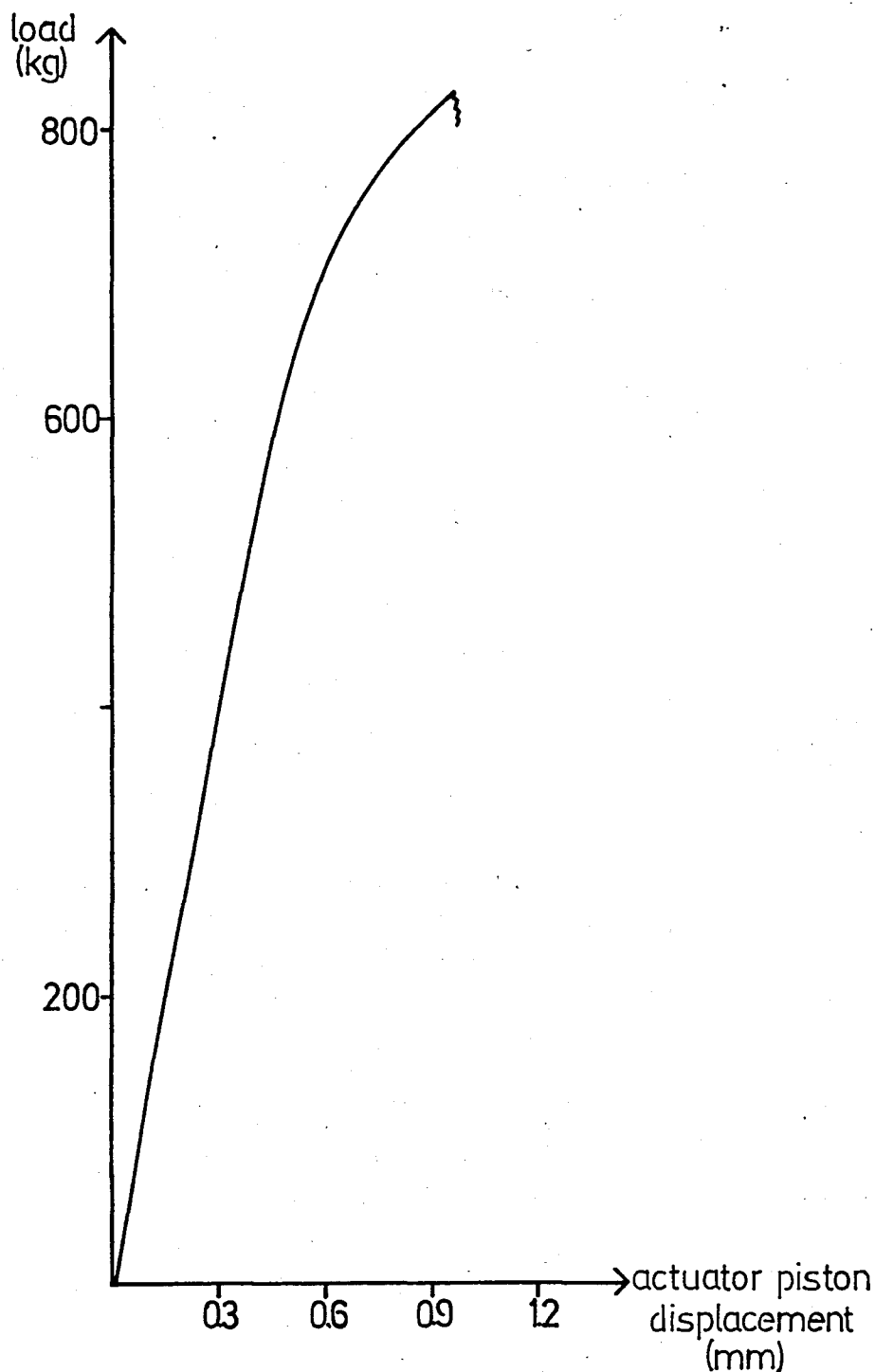


FIGURE 6.1.3- Load vs. displacement behaviour of Specimen 133

Therefore it may be wise to determine E value by using unloading compliance method (i.e: unload the CT specimen at an early stage where no change in crack length is present, then measure the compliance and using elastic bending compliance formula given in Appendix A-4 determine E).

2- BENDING TESTS

a- Experimental setup and specimen preparation

Bending tests were performed by using TPB (three point bend) (see figure 6.2.1) that were machined out from CT specimens 18 and 15.

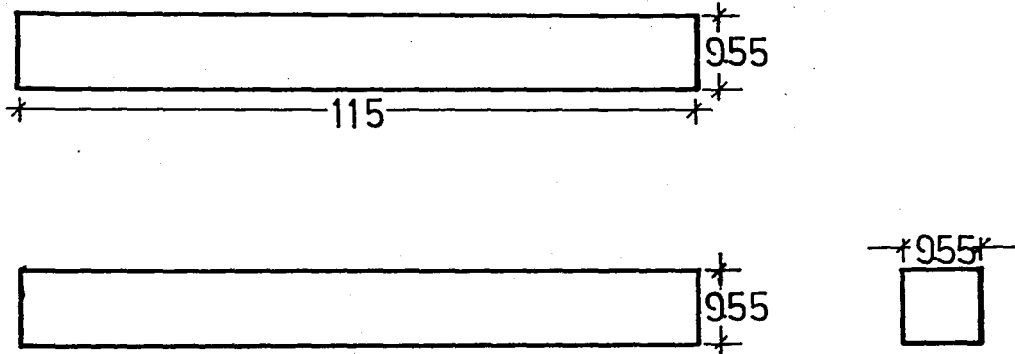


FIGURE 6.2.1-TPB specimen used for bending tests (in mm)

The orientation of bending specimens in CT specimens are as shown in figure 6.1.2 .

Again the MTS fatigue testing machine is used with the appropriate loading apparatus.

b- Experimental Results

Specimens were loaded monotonically until final failure and meanwhile load vs.actuator piston displacement are recorded.

The results are as follows:

SPECIMEN No	P_{\max} (kg)	$S_{ut}^{(2)}$ (kg/mm ²)
115	236	25.7
511	242	26.3
118	224	24.3
181	242	26.3

(2): See Appendix D for calculations

Each of the tests required approximately one minute from zero load to final failure which similar to that of the tensile tests.

c- Analysis and discussion of results

For brittle materials bending tests are of high popularity but one must be aware of the complexities inherent in the test. Compressive strength of gray iron is four times more than the tensile strength consequently, as the moment is increased the neutral axis shifts towards the compression side tending to strengthen the beam (bending stresses do not vary linearly across the section above proportional limit).

Since the behaviour of gray cast iron is highly brittle (see figure 6.2.2) S_{ut} values are calculated by using the simple flexure formula ($\sigma = Mc/I$) and a mean value of 25.6 kg/mm^2 were obtained. This rather high value is not something astonishing because, due to the effect mentioned above the ratio of S_{ut} values obtained from bending and tension tests is usually about 1.8 for cast irons. So it can be deduced that the value of $12-14 \text{ kg/mm}^2$ obtained from the tensile tests is also confirmed by the bending tests (i.e. $25.6/1.8 = 14 \text{ kg/mm}^2$) (5).

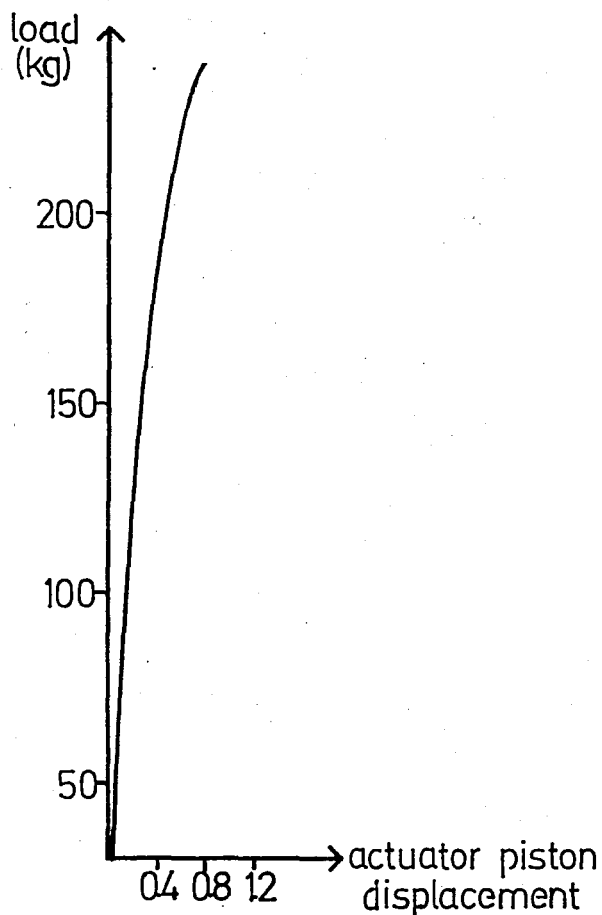


FIGURE 6.2.2- Bending test, load vs. displacement behaviour

In the related literature it is suggested that the speed of testing has the same general effect in the bending test as in tension tests i.e. the greater the speed the higher the indicated strength. So loading rates of the two types of tests are kept similar to obtain consistent results (5).

3- MICROSCOPIC EXAMINATIONS

Apart from the various mechanical property tests a microscopic examination of the specimens are also made. Four specimens of different thickness values are polished and etched by using 5 % Nital (5 % Nitric acid and 95 % Alcohol) as the etchant, then photographs are taken under a microscope.

The obtained photographs are as shown below:



FIGURE 6.3.1- Microstructural view of Specimen 4 (10 mm thick) under 200x magnification.

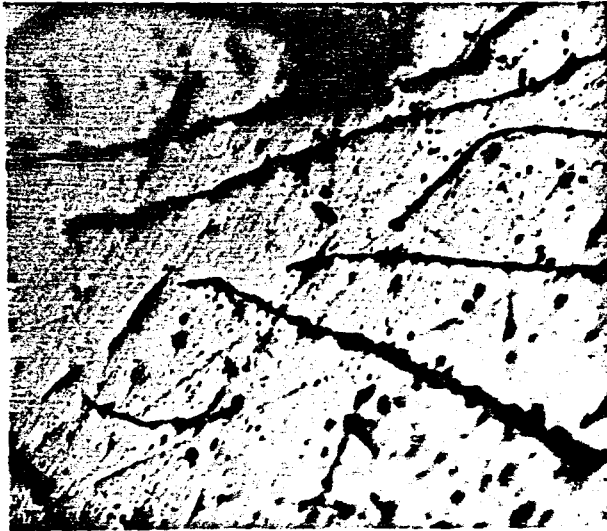


FIGURE 6.3.2- Microstructural view of Specimen 10 (20 mm thick) under 200x magnification.



FIGURE 6.3.3- Microstructural view of Specimen 14 (40 mm thick) under 200x magnification.



FIGURE 6.3.4- Microstructural view of Specimen 25 (40 mm thick) under 200x magnification.

The photographs indicate that the iron in hand is typical gray iron with uniformly distributed randomly oriented graphite flakes and obviously the casting thickness does not affect the graphite flake distribution to a considerable extent (7,12 . Generally material matrix is ferritic and small amounts of pearlite is present usually adjacent to graphite flakes which is the expected outcome of the moderate (to slow) shakeout times of the castings 12 .

4- HARDNESS TESTS

a- Apparatus and specimen preparation

For hardness tests a Rockwell Hardness tester (Wilson Mechanical Instrument co.) was used. This machine had a "Brale" type indenter and was capable of measuring Rockwell A, B, C hardness values which can then be converted to Brinell hardness.

The specimens for the tests are directly obtained from CT specimens and numbered similar to the CT specimen they have been obtained from.

b- Experimental Results and Analysis

A total of five specimens (of three different thickness values) were tested by using a 60 kg load to actuate the penetrator. From each specimen five measurements of different sites were taken, the mean values are as follows:

SPECIMEN No	THICKNESS (mm)	Rockwell A	H _{Br}
6	10	47	140
7	10	43	120
10	20	37	110
14	40	35	100
25	40	42	120

Above values are 15-20 % lower than the published values for ASTM class 20-25 irons following the same trend as the tensile strength values (12).

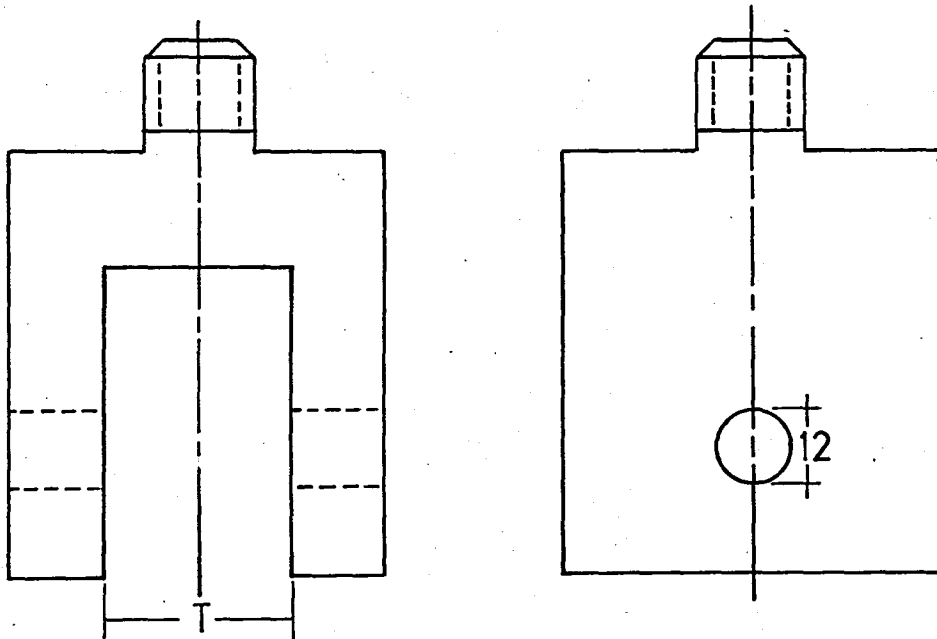
The possible composition alteration for castings of different thicknesses evidently does not affect the hardness values appreciably as suggested by the results.

5- K_{1c} TEST

a- Experimental setup and specimen specifications

For all K_{1c} tests the MTS fatigue testing machine have been used. This machine has a maximum capacity of 10 tons and by the help of it's rather sophisticated hydraulic and electronic control systems it enables the user to perform various tests under load, displacement or strain control.

To couple the specimens with the loading train of the machine two clamps that has been machined out of medium strength steel (see figure 6.5.1) are used.



$T=42$ or 22 mm

FIGURE 6.5.1- Steel clamps used for coupling the compact tension specimens to MTS fatigue testing machine.

All specimens are prepared in the same foundry by using timber cores that are four mm oversized (in all dimensions) than the final intended dimensions of the specimens so that, casting marks can be easily tolerated during machining to the proper size.

Molds were made out of casting sand and all the casting process is performed under same conditions at the same time and one single cupola of molten metal is used in order to achieve a uniform composition for all specimens. Usually the shakeout times are determined intuitively relying on past experience. For this case shakeout times for all the molds were around 25 minutes which is of great importance since for any given gray cast iron composition the rate of cooling from the freezing temperature to below about 640°C determines the ratio of the combined to the graphitic carbon, which controls the hardness and strength of the iron. Too rapid cooling (with respect to carbon and silicon contents) produces "mottled iron" consisting both primary cementite and graphite whilst very slow cooling is likely to produce considerable ferrite as well as pearlite throughout the matrix (12). The desired composition was typical of ASTM class 20-25 gray iron, the details of which are as shown below:

	total Carbon	Silicon	Phosporus	Sulphur	Manganese
%:	3.2	2.3	0.25	0.10	0.6

The castings obtained by the above procedure are then machined by using standard machining equipment (lathe, milling machine) to obtain specimens of dimensions precise upto $1/10$ mm. Three different types of compact tension specimens (CTS) are prepared by varying the thickness but keeping the cross section dimensions constant (see figure 6.5.2).

Before the test specimens are pre-cracked to obtain real sharp crack. The maximum K value during precracking must not exceed $50\% K_{1c}$ so that plastic deformation would not occur (8).

(see Appendix B-2 for a sample pre-crack load estimation).

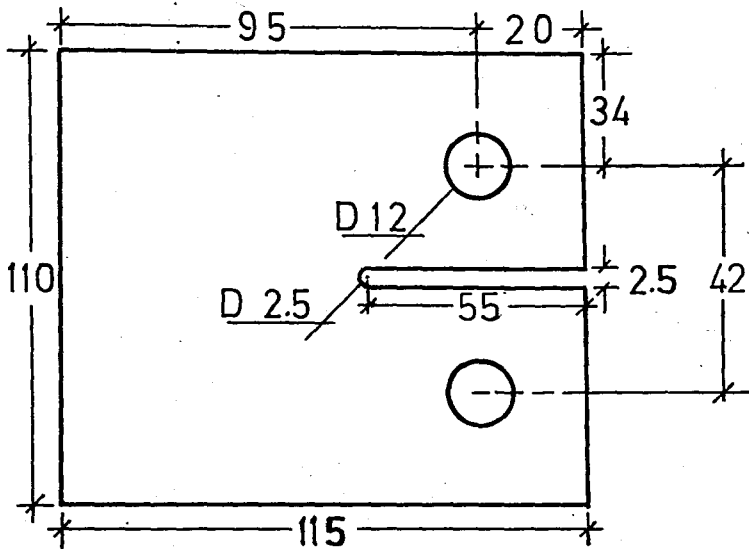


FIGURE 6.5.2- CT specimen for K_{1c} tests (in mm)

For recording the specimen front displacement during loading a clip gage (a cantilever with strain gages) was used and two blades were adhered to the specimen front to hold the gage in proper position (see figure 6.5.3).

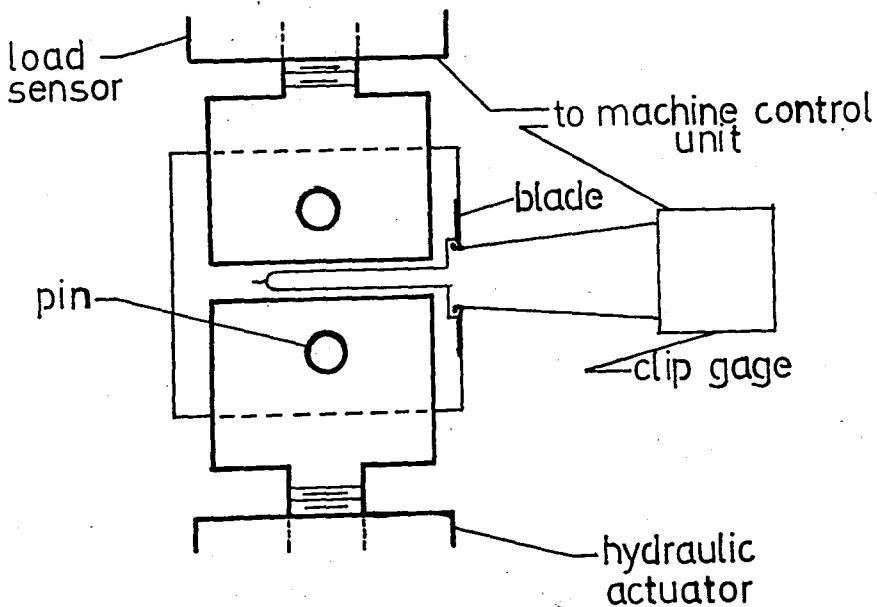


FIGURE 6.5.3- K_{1c} testing setup ready for experiment

As it is shown in figure 6.5.3 specimen front is properly machined so that the blades will be firmly seated in the appropriate place.

b- Experimental Results

Tests were performed by monotonically loading the specimens under stroke control until fracture. whilst load vs. specimen front opening values are recorded by a "Hewlett Packard" X-Y recorder. The results are resumed in the below table:

SPECIMEN No	PRECRACK(mm)	B (mm)	a (mm)	P_{max} (kg)	(3) P_q (kg)	(4) K_q (kg mm ^{-3/2})
1	5.7	10	42.20	755	110	10
2	5.9	10	42.20	760	365	31
10	6.0	20	42.25	1490	450	19.2
14	6.0	40	42.25	3018	370	8
25	0	40	42	3075	920	18.6

(3): see figure 6.5.4 for determination of P_q

(4): see Appendix B-1 for a sample calculation of K_q

c- Analysis and Discussion of Results

Evidently obtained K_q values are not valid because of the violation of the criteria $P_{max}/P_q < 1.1$ and as it's seen in figure 6.5.4 the degree of violation is quite large. Also the K_q data is rather scattered and no improvement is obtained by the use of thicker specimens. These arguments suggest that for gray iron it may not be possible to obtain valid K_{1c} values by using 5 % offset procedure because of the highly nonlinear load vs. displacement behaviour and infact P_q values may be altered by changing the scale of the load vs. displacement plot.

To give a general idea, K_q values obtained by using

$P_q = P_{max}$ are presented below:

SPECIMEN No	B (mm)	P_{max} (kg)	K_q (kg mm ^{-3/2})
1	10	755	64.5
2	10	760	64.8
10	20	1490	63.5
14	40	3018	64.3
25	40	3075	64.8

A brief inspection of the specimens, after failure, indicated that fracture surfaces are rather dark and no appreciable difference is present between the fatigue surface and the fast fracture surface. This fact made the determination of initial crack length difficult and the crack length is determined by carefully watching the crack front with a traveling microscope during fatigue pre-cracking.

To verify the claimed "notch insensitivity" of gray iron specimen 25 is tested without a pre-crack. The result indicates that gray iron is indeed notch insensitive and the obtained value of K_q does not deviate appreciably from the other results however some further tests such as CVN or dynamic tear test may give a better insight of this problem.

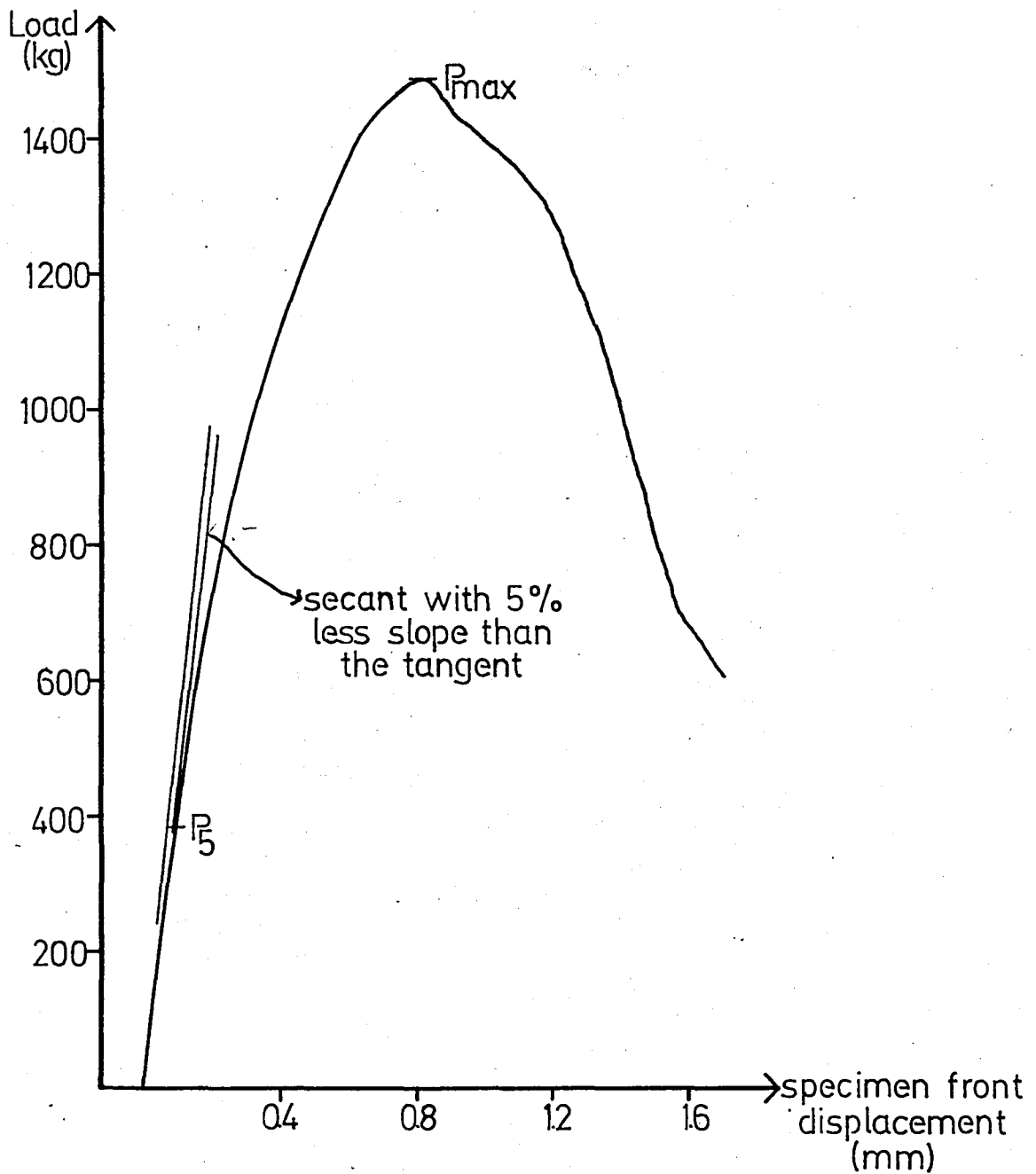


FIGURE 6.5.4- Load vs. displacement plot of Specimen 10 obtained during K_{1c} test.

6- K_{1sc} TEST

a- Experimental Setup and Specimen Preparation

The specimen type used for K_{1sc} tests were three point bend specimen. Necessary number of specimens are machined out from previously used CT specimens (see figure 6.6.1 and 6.1.2).

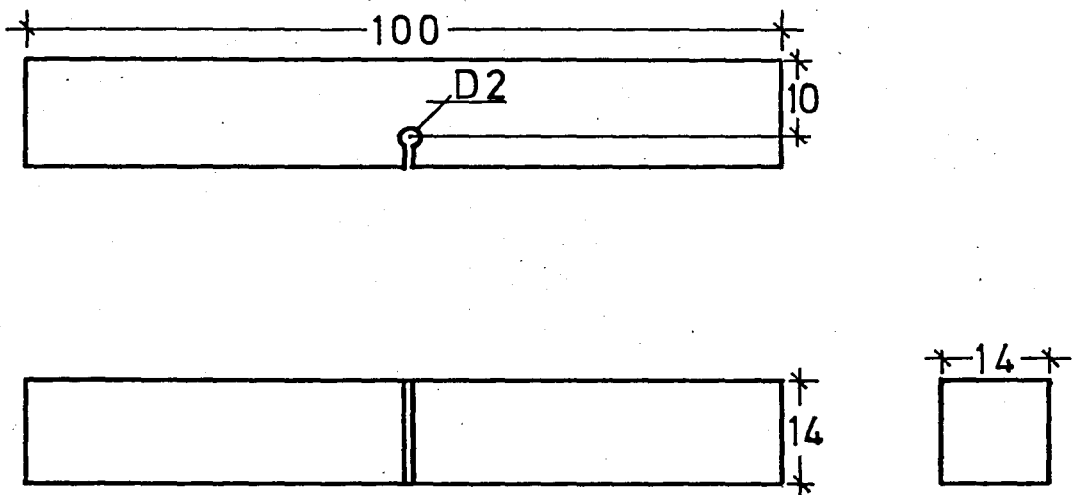


FIGURE 6.6.1- TPB specimen geometry (in mm)

All specimens have been fatigue pre-cracked to obtain a sharp crack and a stress intensity of 45 % K_{1c} (estimated) is used for this purpose so that no plastic yield would occur (see Appendix A-2 for K expressions for TPB and Appendix B-3 for a pre-crack load estimation).

The apparatus that was made use of, for K_{1sc} tests had the capability of simultaneously applying a bending moment to the specimen and exposing it to a corrosive environment (see figure 6.6.2)

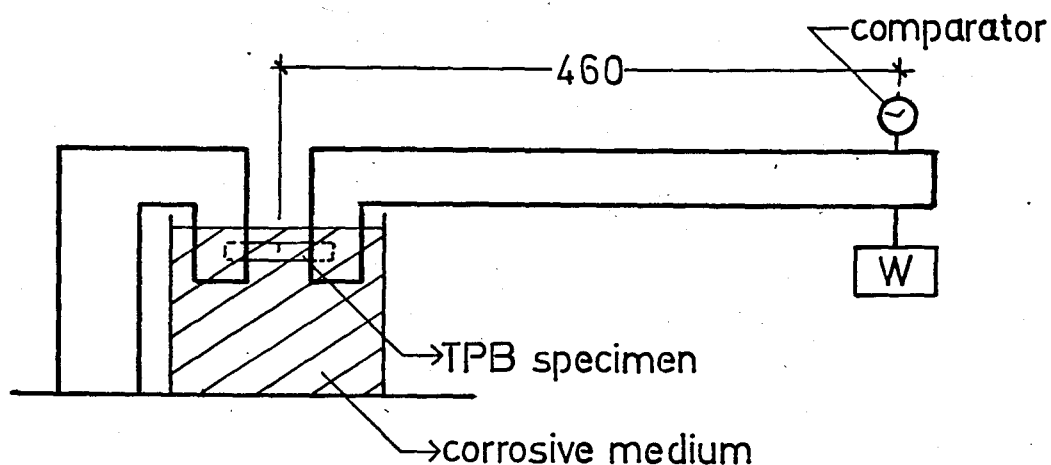


FIGURE 6.6.2- Schematic drawing of K_{1scc} testing apparatus (13)

In order to couple it with the apparatus, the specimen is inserted to the appropriate hole machined for this purpose and then the fixing screws (not show in the figure) are tightened. First the corrosive environment is placed into the proper position and then the weight is increased gradually until it achieves the desired vale.

b- Experimental Results

Experiments have been performed by recording the final failure times starting from the application of the bending moment., In these kind of experiments some creep is observed before final failure and it is usual practice to record this behaviour but since failure times were rather long for this specific case only final failure times are recorded. Alltogether five experiments have been performed by using 10 Normal Sulphuric acid as a corrosive medium.

The obtained results are as follows :

(5) SPECIMEN No	pre-crack (mm)	(6) %K _{1c}	(7) failure time (min)	log time
122	1.6	50	328	2.516
133	1.5	46	528	2.723
313	1.6	40	715	2.854
010	1.6	30	3030	3.481
212	1.5	25	8970	3.953

(5):specimen 122 and 212 are machined out from CT specimen 12 and all the other specimens are numbered accordingly.

(6):see Appendix B-4 for load requirement estimation to generate the desired K_{1c} %.

(7):the difference between the incubation period and the final failure is around 1-2 minutes so only failure times are recorded.

Above results indicate that as the applied moment is decreased incubation periods increased considerably thus verifying the expected trend.After the experiment with 25 % initial K_{1c} specimen 212 is found to be diminished in thickness by 7 %.

c-Analysis and discussion of results

As it is suggested even by a brief inspection of figure 6.6.3 , at K_{1c}/K₁ rates less than 0.3 failure times tend to increase drastically even for a very slight decrease in applied load.

This suggests that ,gray cast iron probably has a definite K_{1scc} in diluted sulphuric acid but unfortunately the decrease in the thickness of specimen 212 avoided the determination of the true K_{1scc} value due to the fact that,a decrease in cross sectional area causes an increase in the applied K_{1c} % thus violating the accuracy of the obtained results.This means that for experiments requiring long testing periods the governing factor that favours failure is,the reduction in specimen dimensions

due to corrosion, rather than stress corrosion effects so, it will be wise to perform these tests with a less concentrated medium which will yield more reliable results.

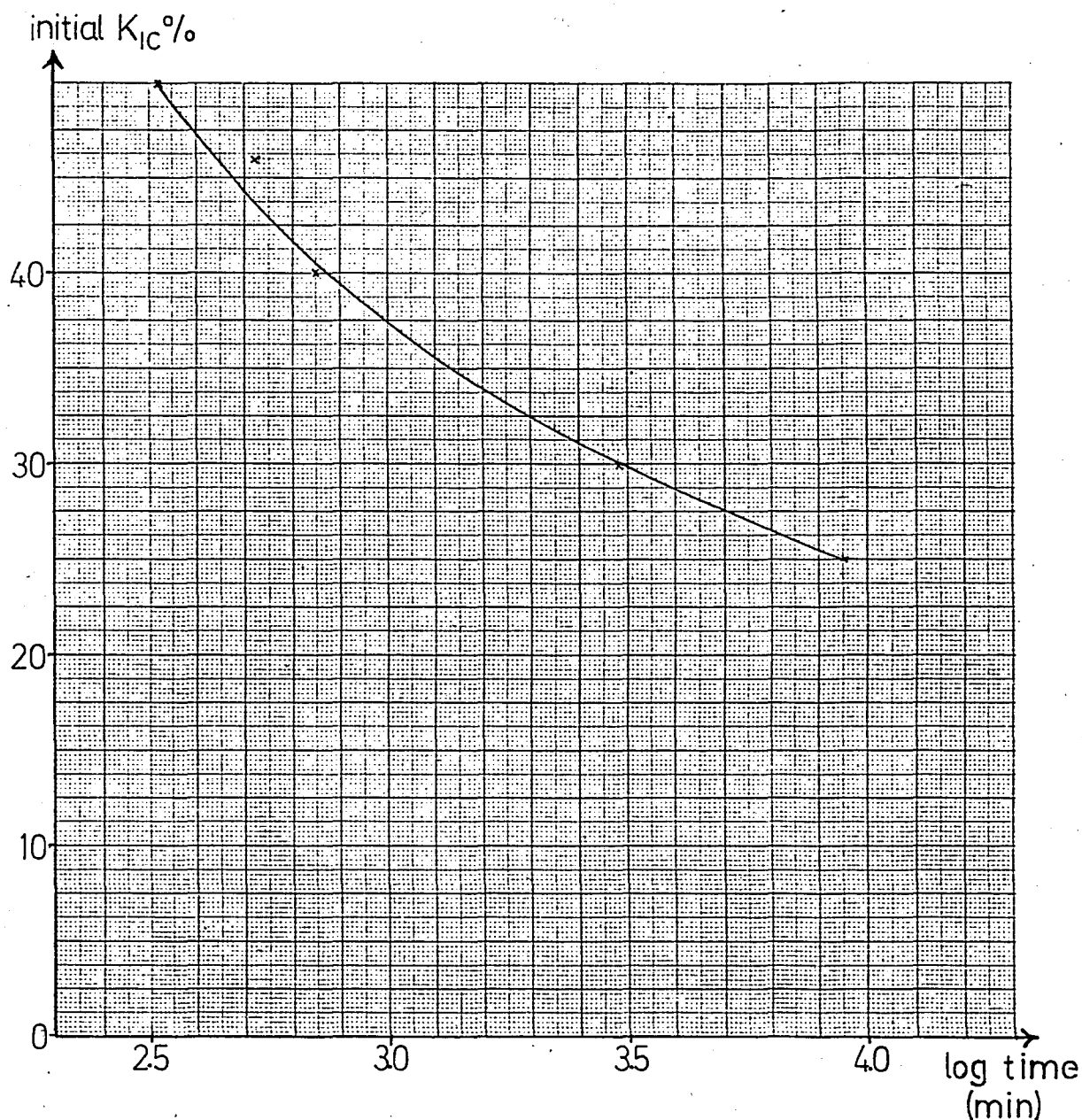


FIGURE 6.6.3- Initial $K_{IC}\%$ vs. log time plot obtained from K_{ISCC} tests

7- FATIGUE TESTS

a-Experimental Setup and Specimen Preparation

For fatigue testing the MTS fatigue testing machine is used. The loading apparatus was similar to that of K_{1c} tests excluding the clip gages (see figure 6.5.3). Before the experiments each specimen were notched by the help of a blade edge, to favour quick initiation. A traveling microscope is used to trace crack propagation (magnification: 32x).

b-Experimental Results

Only 10 mm thick CT specimens are tested and four experiments are performed with a loading rate of 10 Hz. All the tests are conducted under load control. Change in crack length with respect to number of cycles are recorded during each experiment. Specimens 5 and 6 are used for observing the tension to tension fatigue behaviour starting with a ΔK of $19.5 \text{ kg mm}^{-3/2}$ and the final fracture occurring at a stress intensity of $60 \text{ kg mm}^{-3/2}$.

Specimens 7 and 18 are also fatigue tested by starting with a ΔK of $26.3 \text{ kg mm}^{-3/2}$ but this time the load is reduced by $3/4$ at $\Delta K \approx 35 \text{ kg mm}^{-3/2}$ so that crack closure effects could be observed. The results are resumed in figures 6.7.1 (a,b,c) and in Appendix C-1 and C-3.

c- Analysis and Discussion of Results

A brief inspection of the data indicates that, below a ΔK value of $23\text{-}24 \text{ kg mm}^{-3/2}$ the propagation rates are rather unpredictable and scattered (so they are excluded in the graphs) and this interesting trend is observed both in specimens 5 and 6.

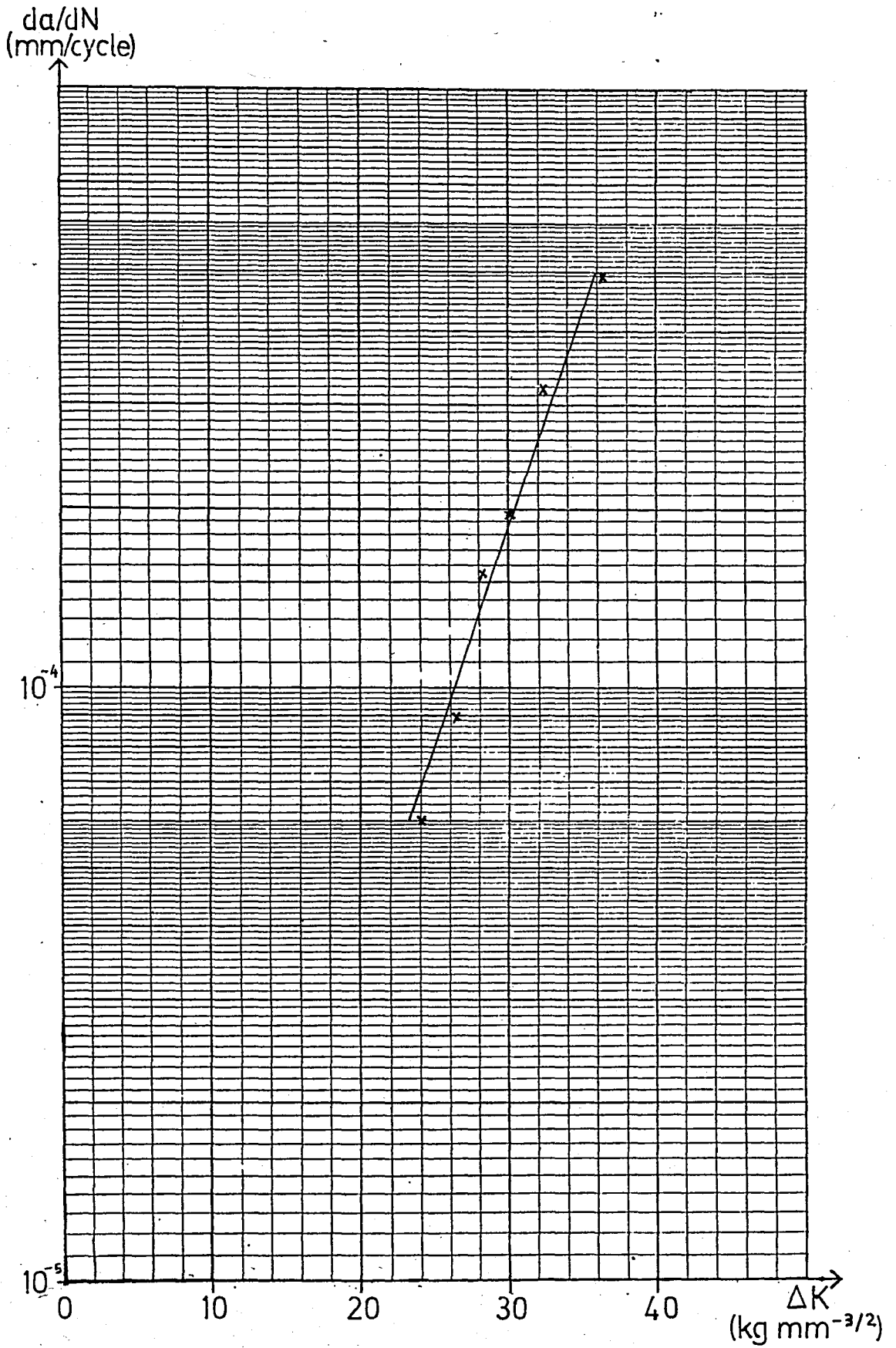


FIGURE 6.7.1(a)- da/dN vs. ΔK behaviour of Specimen 5.

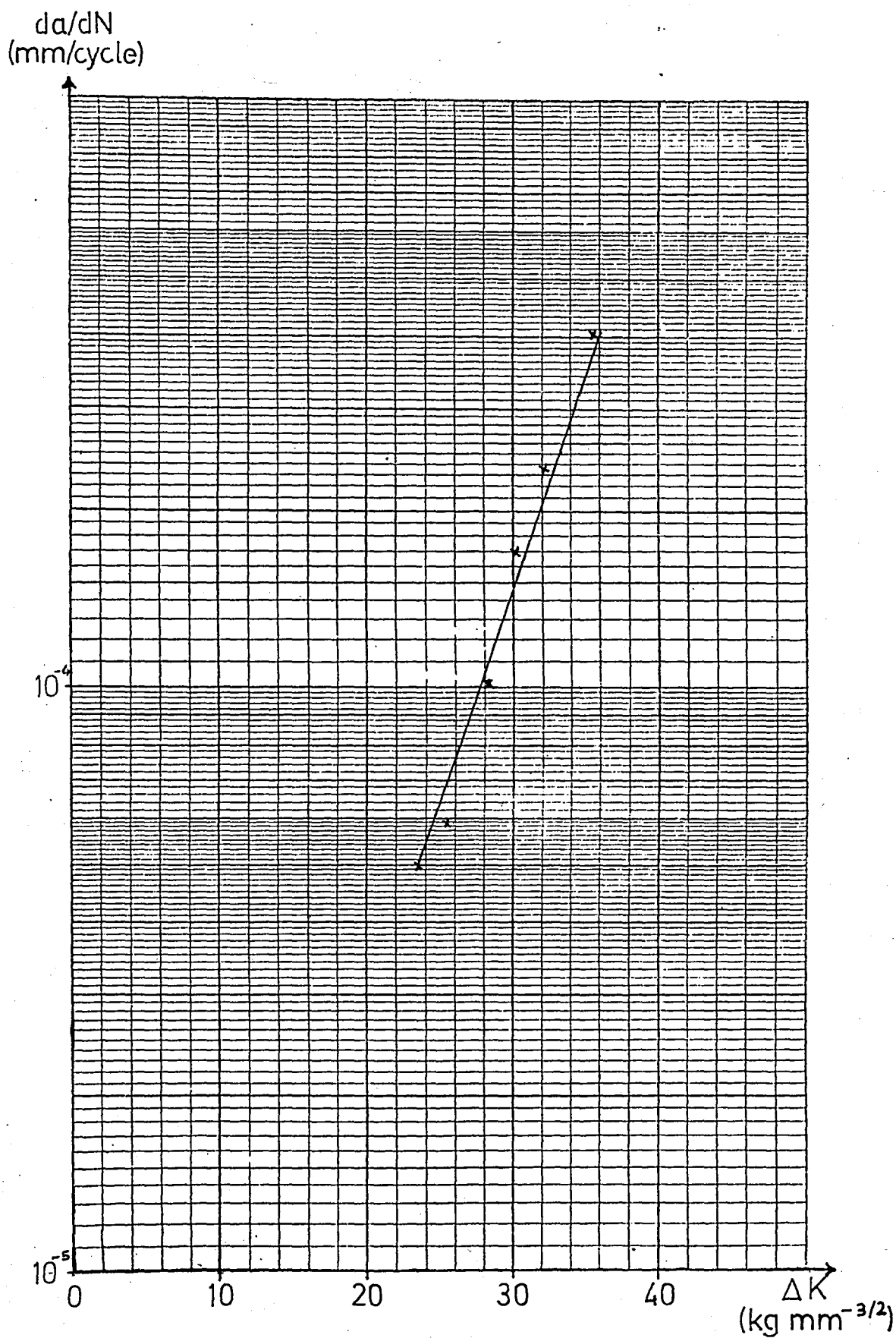


FIGURE 6.7.1(b)- da/dN vs. ΔK behaviour of Specimen 6 .

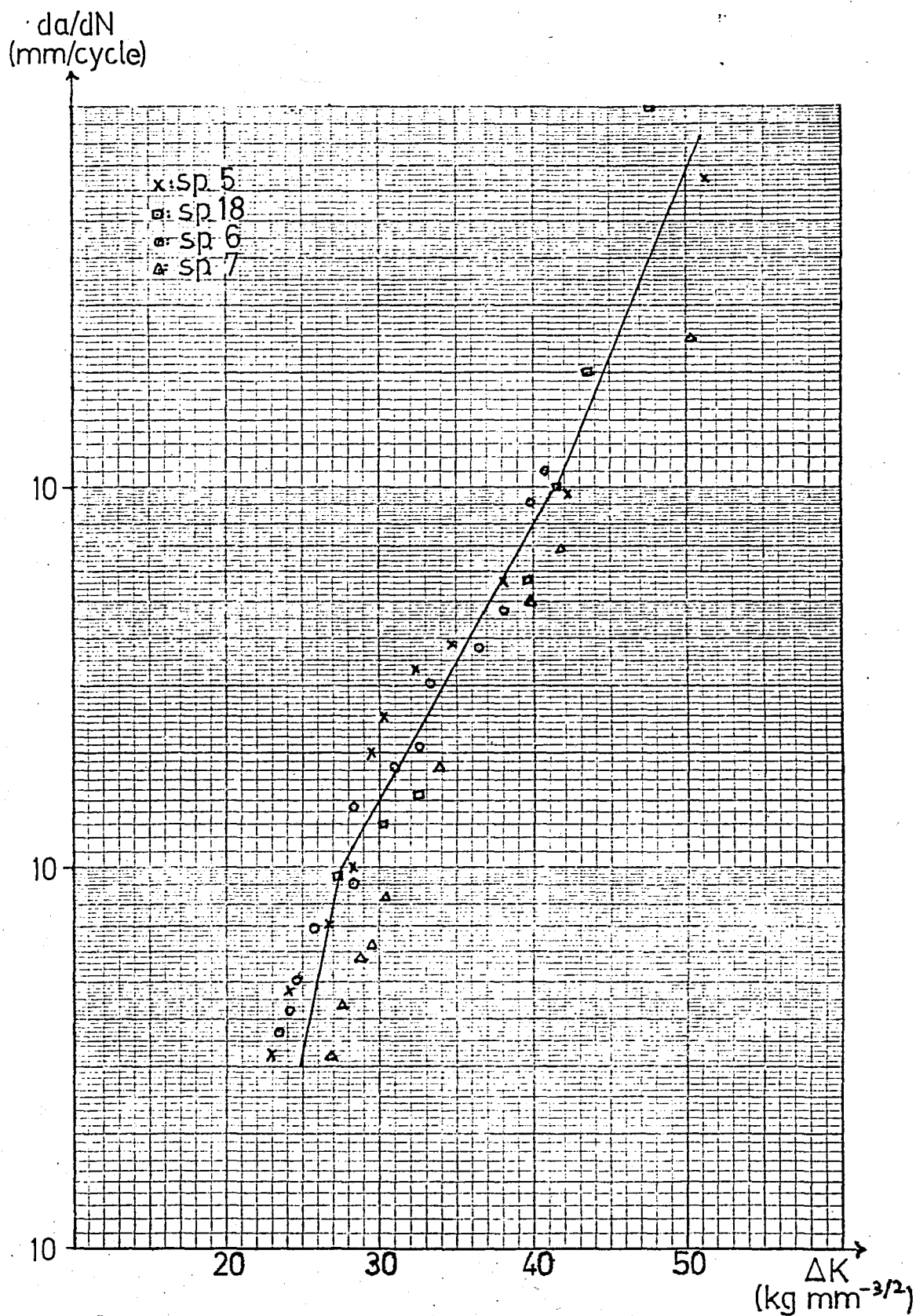


FIGURE 6.7.1(c)- Combined da/dN vs. ΔK behaviour of Specimens 5, 6, 7 and 18 .

While testing Specimen 6 crack propagation suddenly stopped at $a=2.3\text{mm}$ and it required approximately 10^6 cycles to pass that region. Similar trends are also noticed in specimen 5 though in a less pronounced form, at $a=16.1\text{mm}$ and 17.1mm . This sudden propagation retardation is most probably due to void formation around some non metallic inclusions (such as graphite or sulphur) in the material matrix that lies in front of the crack tip (9,11). Certainly this is only an assumption and a tangible explanation may require some further microscopic study.

The reduction of load by $3/4$ caused a considerable crack retardation for the first one mm after the reduction and this is in harmony with the behaviour suggested by the related literature.

Some simple calculations using figures 6.7.1(a) and (b) yields the constant m of the Paris equation as 5.6 and the constant C as 1.2×10^{-12} for region II. Similarly by using the combined plot of all the specimens (figure 6.7.1(c)) m is calculated to be 5.7 (see Appendix C-2 for a sample calculation of m and c). The unpredictable propagation retardation mentioned above is not included in the calculation of m which, if included would yield lower m values. This rather high value of m (it is usually around 3-4) indicates the rather unreliable fatigue behaviour of gray cast iron which is in accordance with the general opinions about this material.

No fatigue marks or visible striations are observed on the fracture surface of the specimens and it is difficult to understand the crack length at final failure because there is no visible differences between the fatigue surface and the fast fracture surface. The explanation for this unusual behaviour may require

some further study.

8- J_1 TEST

a- Experimental Setup and specimen preparation

For J_1 tests again MTS fatigue testing machine is used. Specimens are Compact tension specimens with knife edges on the specimen front (see figure 6.5.3) and no notch was present at the crack tip.

b- Experimental Results and Analysis

Experiments are performed by monotonically loading the specimens until a specific value and then by unloading slowly whilst load vs. crack front displacement is recorded. This procedure is conducted several times and each time unloading compliance is measured (see figure 6.8.1) Which is then used for predicting crack advance (see Appendix A-4). Afterwards by using equation (6) J values corresponding to different crack length are obtained 15 .

$$J = \frac{(1+\alpha)}{(1+\alpha^2)} (2A/Bb) \quad (6)$$

Where A: Area under load-displacement curve.

B: Specimen thickness.

b: uncracked ligament.

$$\alpha = ((2(a/W)^2 + 2)^{1/2} - (1 + a/w)) / (1 - a/W)$$

Obtained results using the above procedure are resumed in figure 6.8.2 .

Also by inserting the elastic unloading compliance values into equation (10) one can obtain elastic modulus from CT specimens.

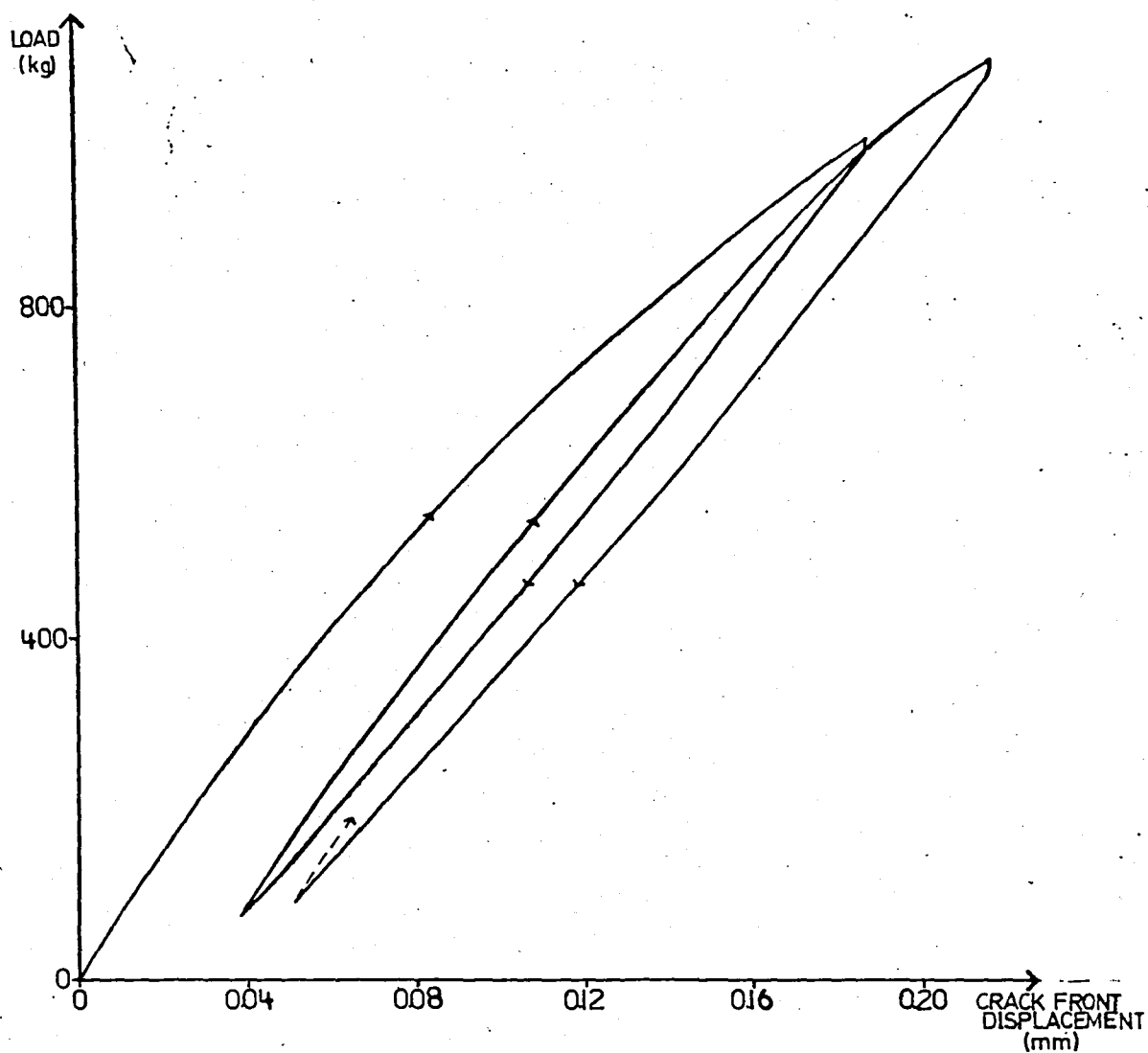


FIGURE 6.8.1- Load vs. displacement plot obtained from J_1 test

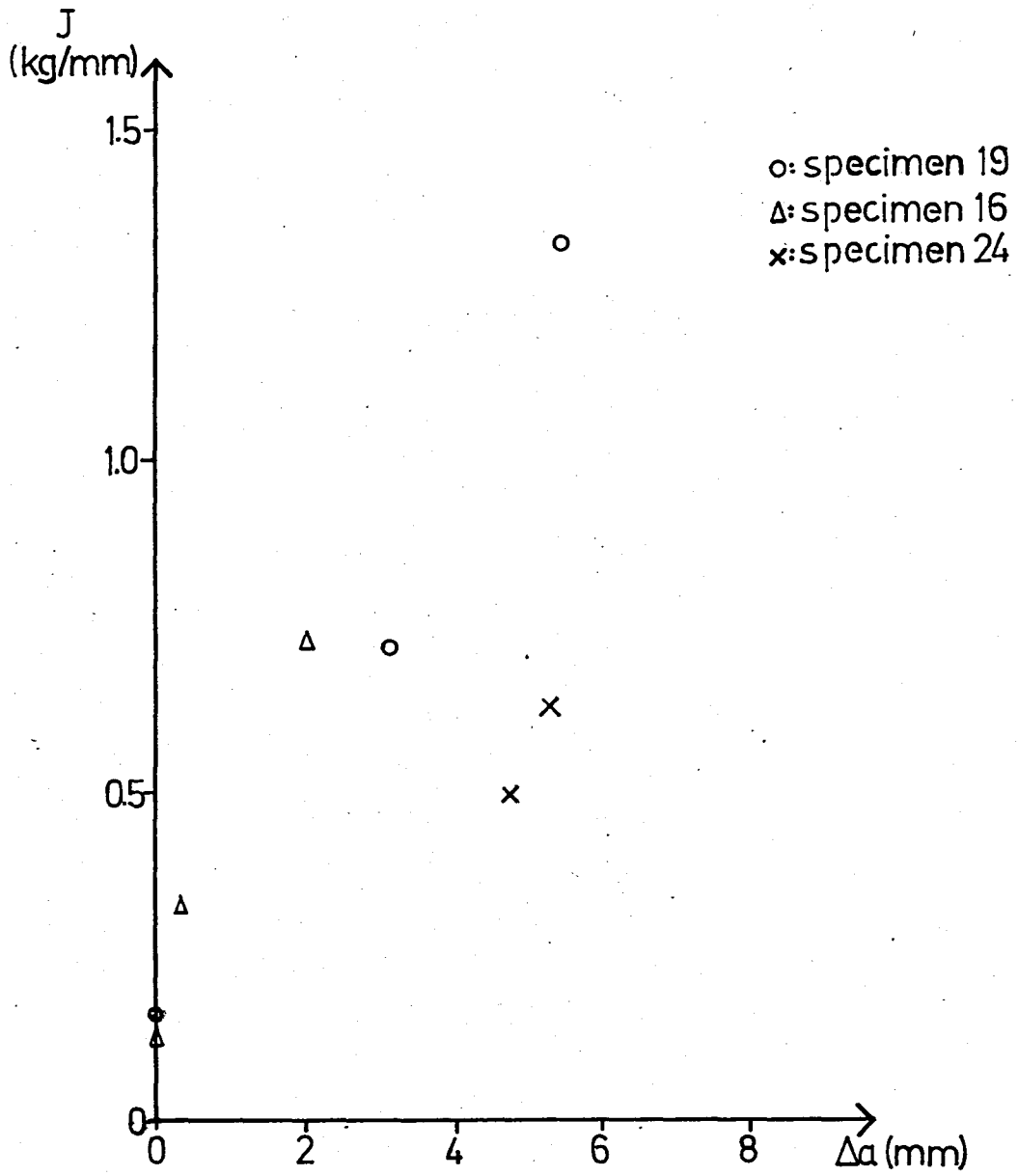


FIGURE 6.8.2- J vs. Δa plot of Specimens 16, 19 and 24

Below are the E values obtained by using equation (10):

SPECIMEN No	THICKNESS	E (kg/mm ²)
16	10	8800
17	10	8000
19	10	8800
24	10	9100

Obviously both the J and E values are scattered and to obtain eligible results it may be necessary to use more consistent specimens (with each other) with slightly different geometries.

CHAPTER VII

CONCLUSIONS

After concluding all the tests it can be deduced that gray iron is a rather impotent material that behaves in an extremely untrustworthy manner, under static or dynamic tensile loading conditions.

Microstructural analysis indicates that the material matrix is composed of fine graphite flakes distributed randomly in ferrite and small amount of pearlite.

A Brinell hardness value of 120 and a ultimate tensile stress of $12-14 \text{ kg/mm}^2$ is the outcome of the mechanical tests and obviously these values are rather low.

A valid K_{1c} value could'nt be obtained and satisfying plane strain requirements while using 5 % offset technique proved to be quite difficult and use of thicker specimens probably will not make much of a change. Developing a different technique for the interpretation of K_q data of gray iron may be both interesting and usefull.

Sulphuric acid (10 Normal) proved to be a rather strong corrodent for gray iron and as the results suggests, there may be a K_{1scc} value in much weaker environments where stress corrosion is the dominant factor in failure rather than the corrosion itself.

Fatigue tests indicated that the constant "m" of the Paris equation is around 5.5 (which is a bit higher than the usual value of 3-4) thus proveing the weak fatigue behaviour of gray iron in a quantitative sense.

A point that is of considerable interest is the unpredictable fatigue crack retardation posed by some specimens due to some unknown microstructural obstacles on the crack front and further studies on this subject may intend to generate these obstacles throughout the whole matrix consequently developing a more fatigue resistant material.

Above discussions confirm the general contentment that "use of gray iron should be avoided under tensile stresses" and further studies on fracture properties of this metal will probably be of academic interest rather than having a significant practical value.

APPENDIX A

(A-1) - Westergaard stresses in the vicinity of crack tip for

Mode I type loading:

$$\sigma_x = \frac{K_I}{(2\pi r)^{1/2}} \cos(\theta/2) (1 - \sin(\theta/2) \sin(3\theta/2))$$

$$\sigma_y = \frac{K_I}{(2\pi r)^{1/2}} \cos(\theta/2) (1 + \sin(\theta/2) \sin(3\theta/2))$$

$$\tau_{xy} = \frac{K_I}{(2\pi r)^{1/2}} \sin(\theta/2) \cos(\theta/2) \sin(3\theta/2)$$

(A-2) - K_q expression for ASTM compact tension specimen:

$$K_q = \frac{P_q}{BW^{1/2}} f(a/W) \quad (7)$$

$$f(a/W) = 29.6(a/W)^{1/2} - 185.5(a/W)^{3/2} + 655.7(a/W)^{5/2} - 1017(a/W)^{7/2} + 638.9(a/W)^{9/2}$$

Where B: thickness of specimen (inches)

W: width of specimen (inches)

a: crack length (inches)

(A-3)- K_q expression for ASTM TPB specimen

$$K_q = \frac{P_q S}{BW^{3/2}} f(a/W) \quad (8)$$

$$f(a/W) = 2.9(a/W)^{1/2} - 4.6(a/W)^{3/2} + 21.8(a/W)^{5/2} - 37.6(a/W)^{7/2} + 38.7(a/W)^{9/2}$$

Where B: thickness of specimen (inches)

W: dept of specimen (inches)

S: span length (inches)

a: crack length (inches)

Another expression which relates bending moment to K_1 is as follows (13):

$$K_1 = \frac{4.12 m (\alpha^{-3} - \alpha^3)^{1/2}}{B W^{3/2}} \quad (9)$$

Where m: bending moment at the crack plane

α : $1 - (a/W)$

(A-4)- Tentative test procedure for determining plane strain J_1 -R curve:

First load the specimen until a specific level and then unload to measure elastic unloading compliance. Repeat this procedure for several times and then use the below formulas to obtain J_1 values corresponding to different crack lengths.

$$a/W = 1.000196 - 4.06319 u_{LL} + 11.242 u_{LL}^2 - 106.043 u_{LL}^3 + 464.335 u_{LL}^4 - 650.677 u_{LL}^5 \quad (10)$$

Where $u_{LL} = \frac{1}{(BE \delta/P)^{1/2} + 1}$

δ/P = specimen elastic compliance on an unloading

δ = increment of load line displacement

P = increment of applied load corresponding to δ

E = elastic modulus

$$J_{i+1} = (J_i + (\eta/b)_i (A_{i,i+1}/B)) \cdot (1 - (\gamma/b)_i a) \quad (11)$$

Where $\eta = 2 + 0.522 b/W$

$\gamma = 1 + 0.76 b/W$

A = area under load vs. load line displacement.

b = uncracked ligament.

Using equation (10) change in crack length can be calculated which can then be inserted into equation (11) to determine J_1 .

APPENDIX B

(B-1)- Sample K_q calculation for CTS :

$a=42\text{mm}$ (with pre-crack)

$W=95\text{mm}$

$a/W=0.445$

$f(a/W)=8.22$

$B=10\text{mm}$

$P_q=365\text{ kg}$ (for Specimen 2)

$$K_q = \frac{P_q}{B W^{1/2}} f(a/w)$$

$$K_q = \frac{365}{10 \times 95^{1/2}} 8.22 = 31 \text{ kg mm}^{-3/2}$$

(B-2)- Fatigue pre-crack load estimation for CTS:

$$a=42.2\text{mm}$$

$$W=95\text{mm}$$

$$a/W=0.445$$

$$B=20\text{mm (for specimen 10)}$$

$$K=58 \text{ kg mm}^{-3/2} \text{ (estimated by using } P_q=90 \% P_{\max})$$

$$f(a/W)=8.22$$

Using equation (7):

$$58 = \frac{P}{20 \times 95^{1/2}} \cdot 8.22$$

$$P=1350 \text{ kg}$$

$$\text{Precrack load}=50 \% P=675 \text{ kg}$$

(B-3)- TPB precrack load estimation:

$a=6.5\text{mm}$ (with pre-crack)

$W=14\text{mm}$

$a/W=0.46$

$f(a/W)=2.35$

$K=58 \text{ kg mm}^{-3/2}$ (estimated by using $P_q=90 \% P_{\max}$)

$S(\text{span length})=52\text{mm}$

Using equation (8):

$$58 = \frac{P \times 52}{20 \times 14^{3/2}} \times 2.35$$

$P=275 \text{ kg}$

Pre-crack load $= 50 \% P = 130 \text{ kg}$

(B-4)- Sample calculation for load requirement to generate the desired K_{1c} % for TPB specimens:

$$a=6.5 \text{ mm (with pre-crack)}$$

$$B=14 \text{ mm}$$

$$W=14 \text{ mm}$$

$$a/W=0.46$$

$$\alpha=1-a/W=0.54$$

$$\text{moment arm}=460 \text{ mm}$$

$$m=460 P$$

$$K_{1c}=58 \text{ kg mm}^{-3/2} \text{ (estimated by using } P_q=90 \% P_{\max})$$

Using equation (9) yields:

$$P_{\max}=8.9 \text{ kg}$$

To generate 50 % K_{1c} use 50 % $P_{\max}=4.5 \text{ kg}$

The weight of the fixing arm and the weight hanger acts as a 2.8 kg weight in the load line, so the weight that must be added is:

$$4.5-2.8=1.7 \text{ kg}$$

APPENDIX C

(C-1)- Data obtained from fatigue tests are as follows:

Specimen 5 ($P_{\min}=30$ kg , $P_{\max}=300$ kg) .

$\Delta a(\text{mm})$	#of cycles $\times 10^3$	ΔK ($\text{kg mm}^{-3/2}$)	da/dN (mm/cycle)
0	0	19.50	0
0.8	7.6	19.95	10.5×10^{-5}
1.6	15.0	20.42	10.8×10^{-5}
2.2	30.0	20.51	40.0×10^{-6}
3.3	45.0	21.40	73.3×10^{-6}
4.5	55.0	21.90	12.0×10^{-5}
5.5	73.0	22.40	55.5×10^{-6}
6.5	104.0	22.90	32.0×10^{-6}
7.5	125.0	24.00	47.6×10^{-6}
8.5	144.0	24.50	52.6×10^{-6}
9.5	158.0	25.10	71.4×10^{-6}
10.5	172.0	25.70	71.5×10^{-6}
12.1	187.0	27.50	10.6×10^{-5}
13.1	197.0	28.20	12.0×10^{-5}
14.1	202.0	29.50	20.0×10^{-5}
15.1	206.0	30.20	25.0×10^{-5}
16.1	211.5	31.60	22.2×10^{-5}
17.1	214.5	32.40	33.3×10^{-5}
18.1	217.8	33.92	30.5×10^{-5}
19.1	220.4	34.70	38.4×10^{-5}
20.1	223.2	36.30	40.3×10^{-5}
21.1	225.0	38.00	56.4×10^{-5}
23.8	227.8	42.22	96.4×10^{-5}
27.7	228.4	51.30	65.0×10^{-4}
29.9	228.5	58.90	27.5×10^{-3}
Failure			

In the above table da/dN values are calculated by by using a least squares method to fit a curve to a $\log a$ vs. $\log N$ plot and then by by differentiating to obtain the slope.

Specimen 6 ($P_{\min}=30$ kg, $P_{\max}=300$ kg) .

Δa (mm)	# of cycles $\times 10^3$	ΔK (kg mm $^{-3/2}$)	da/dN (mm/cycle)
0.0	0.0	19.5	0.0
1.0	10.7	20.0	93.5×10^{-6}
2.0	32.5	20.4	45.9×10^{-6}
2.3	874.5	20.6	36.0×10^{-8}
2.8	1466.8	20.9	84.0×10^{-8}
3.4	1601.0	21.4	74.5×10^{-7}
4.8	1838.5	21.9	42.0×10^{-7}
5.8	2178.3	22.4	35.0×10^{-7}
6.8	2205.3	23.4	37.0×10^{-6}
7.8	2229.0	24.0	42.2×10^{-6}
8.8	2248.7	24.5	50.7×10^{-6}
9.8	2263.0	25.7	69.9×10^{-6}
10.8	2278.0	26.3	66.6×10^{-6}
11.8	2300.0	26.9	45.5×10^{-6}
12.8	2311.0	28.2	90.9×10^{-6}
13.8	2317.9	29.3	14.5×10^{-5}
14.8	2325.0	30.2	18.2×10^{-5}
15.8	2330.5	30.9	20.8×10^{-5}
16.8	2335.3	32.4	23.4×10^{-5}
17.8	2338.6	33.1	30.3×10^{-5}
18.8	2342.1	34.7	28.6×10^{-5}
19.9	2345.0	36.3	37.9×10^{-5}
20.9	2347.1	38.0	47.6×10^{-5}
21.9	2348.2	39.8	90.9×10^{-5}
22.9	2349.1	40.7	11.1×10^{-4}
23.9	2350.9	42.7	11.2×10^{-4}
30.3	2350.9	59.0	71.1×10^{-4}
Failure			

Specimen 7 (Initially $P_{\min}=30$ kg, $P_{\max}=400$ kg, then at $a=9.5$ mm P_{\max} is reduced to 300 kg and at $a=16.6$ mm it is reduced to 200 kg which retarded the crack indefinitely so P_{\max} is reduced to 300 kg again)

Δa (mm)	#cycles $\times 10^3$	ΔK (kg mm $^{-3/2}$)	da/dN (mm/cycle)
0.0	0.0	26.3	0.0
2.5	78.0	28.2	32.0×10^{-6}
3.5	94.5	28.8	60.6×10^{-6}
4.5	99.0	30.2	22.2×10^{-5}
5.5	104.0	30.9	20.0×10^{-5}
6.5	112.0	31.6	12.5×10^{-5}
8.5	116.3	33.9	46.5×10^{-5}
9.5	119.4	34.7	31.7×10^{-5}
10.5	208.0	25.7	11.3×10^{-6}
11.6	242.0	26.9	32.3×10^{-6}
12.6	265.0	27.5	43.4×10^{-6}
13.7	284.0	28.8	58.0×10^{-6}
14.7	300.0	29.5	62.5×10^{-6}
15.7	312.0	30.9	83.3×10^{-6}
16.6	330.0	31.6	60.0×10^{-6}
16.6	1185.5	20.0	0.0
17.0	1191.0	32.4	72.8×10^{-6}
18.0	1196.5	33.9	18.2×10^{-5}
19.0	1202.0	34.7	19.0×10^{-5}
20.0	1207.9	36.3	19.6×10^{-5}
21.0	1214.0	38.0	19.0×10^{-5}
22.0	1216.0	39.8	50.0×10^{-5}
23.0	1217.4	41.7	69.4×10^{-5}
27.0	1219.1	50.1	24.5×10^{-4}
28.0	1219.2	52.5	25.0×10^{-3}
Failure			

Specimen 18 (Initially $P_{\min}=30$ kg, $P_{\max}=400$ kg, then at $a=10$ mm P_{\max} is reduced to 300 kg) .

Δa (mm)	#Cycles $\times 10^3$	ΔK (kg mm $^{-3/2}$)	da/dN (mm/cycle)
0	0.0	26.6	0.0
1	6.0	27.3	16.7×10^{-5}
2	10.0	28.0	25.0×10^{-5}
3	14.0	28.7	25.5×10^{-5}
4	18.0	29.5	25.0×10^{-5}
5	22.5	30.3	22.2×10^{-5}
6	27.0	31.2	22.0×10^{-5}
7	31.0	32.1	26.0×10^{-5}
8	34.5	33.0	28.6×10^{-5}
9	37.0	34.0	40.0×10^{-5}
10	39.0	35.1	50.0×10^{-5}
11	170.0	26.4	76.0×10^{-7}
12	180.5	27.2	95.0×10^{-6}
13	193.0	28.1	89.0×10^{-6}
14	205.0	29.1	93.3×10^{-6}
15	212.6	30.1	13.0×10^{-5}
17	225.5	32.4	15.5×10^{-5}
22	234.3	39.6	57.0×10^{-5}
23	235.3	41.4	10.0×10^{-4}
24	235.8	43.3	20.0×10^{-4}
25	236.1	45.4	33.0×10^{-4}
26	236.2	47.6	10.0×10^{-3}
Failure			

(C-2)- Calculation of constants "c" and "m" of Paris equation:

Taking logarithms of both sides of equation (2) yields:

$$\log (da/dN) = \log C + m \log \Delta K$$

So "m" can be found by obtaining the slope of 6.7.1 .

For Specimen 5 :

By using figure 6.7.1(a)

$$m = (\log 10^{-3} - \log 10^{-4}) / (\log 40 - \log 26.5) = 5.5$$

Similarly for Specimen 6 $m = 5.7$

Inserting $m = 5.5$ into the main equation and inserting a few points from the graph yields an average value of 1.2×10^{-12} for the proportionality constant C .

(C-3)- a vs. #cycles curves obtained from fatigue tests:

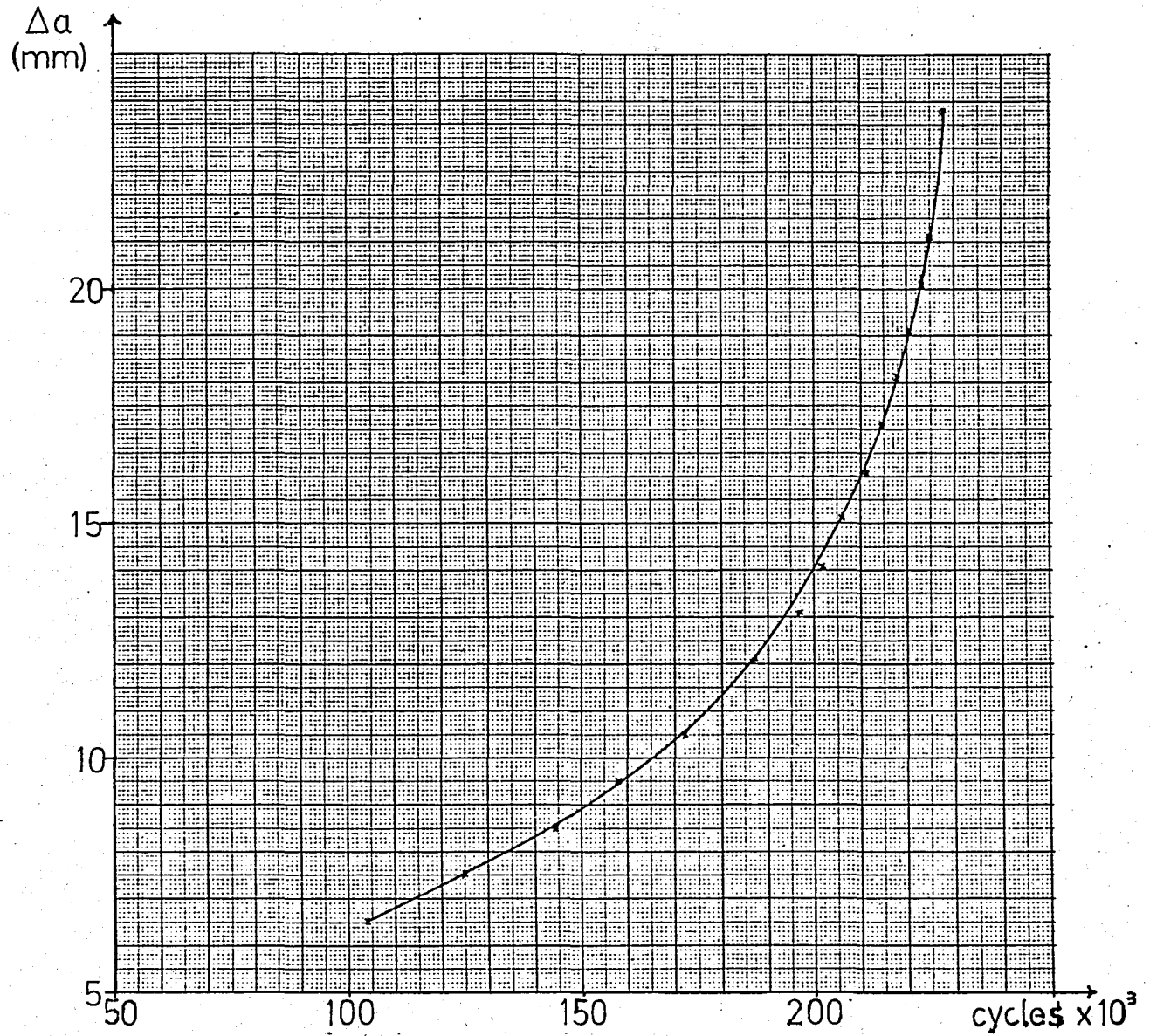


FIGURE 7.1- Fatigue behaviour of Specimen 5

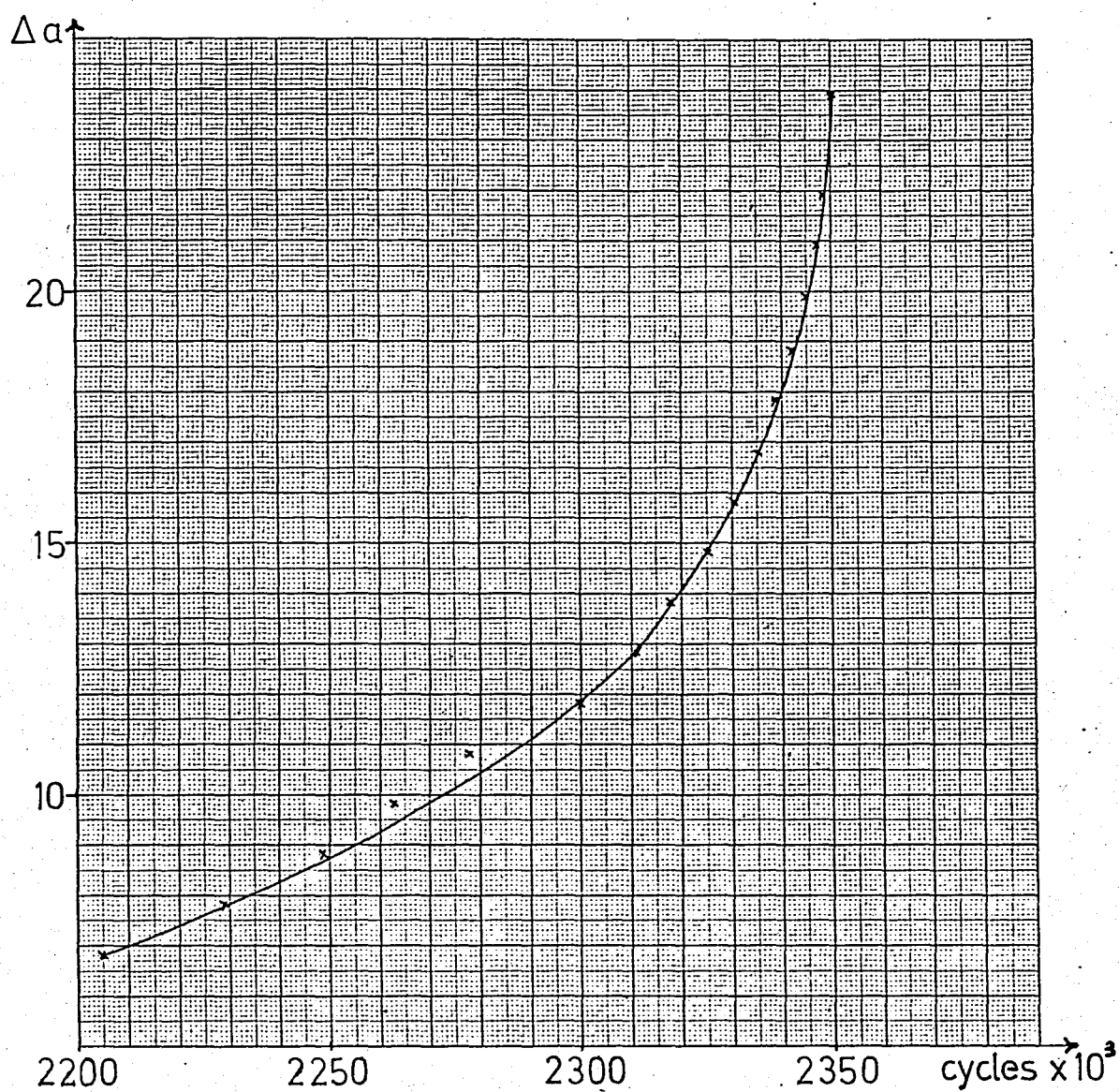


FIGURE 7.2- Fatigue behaviour of Specimen 6

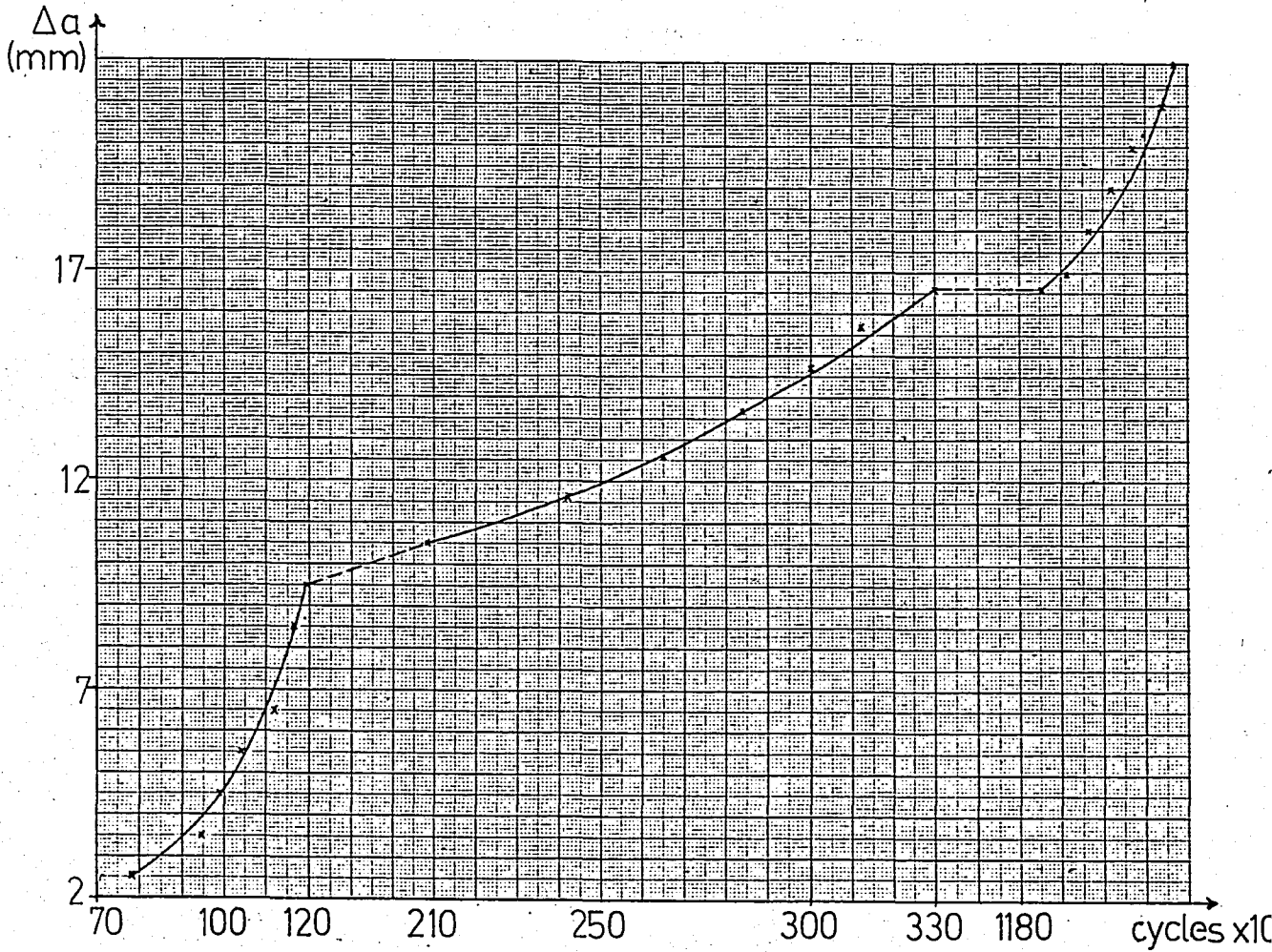


FIGURE 7.3- Fatigue behaviour of Specimen 7 (dotted zones indicate the crack retardation due to reduction in load)

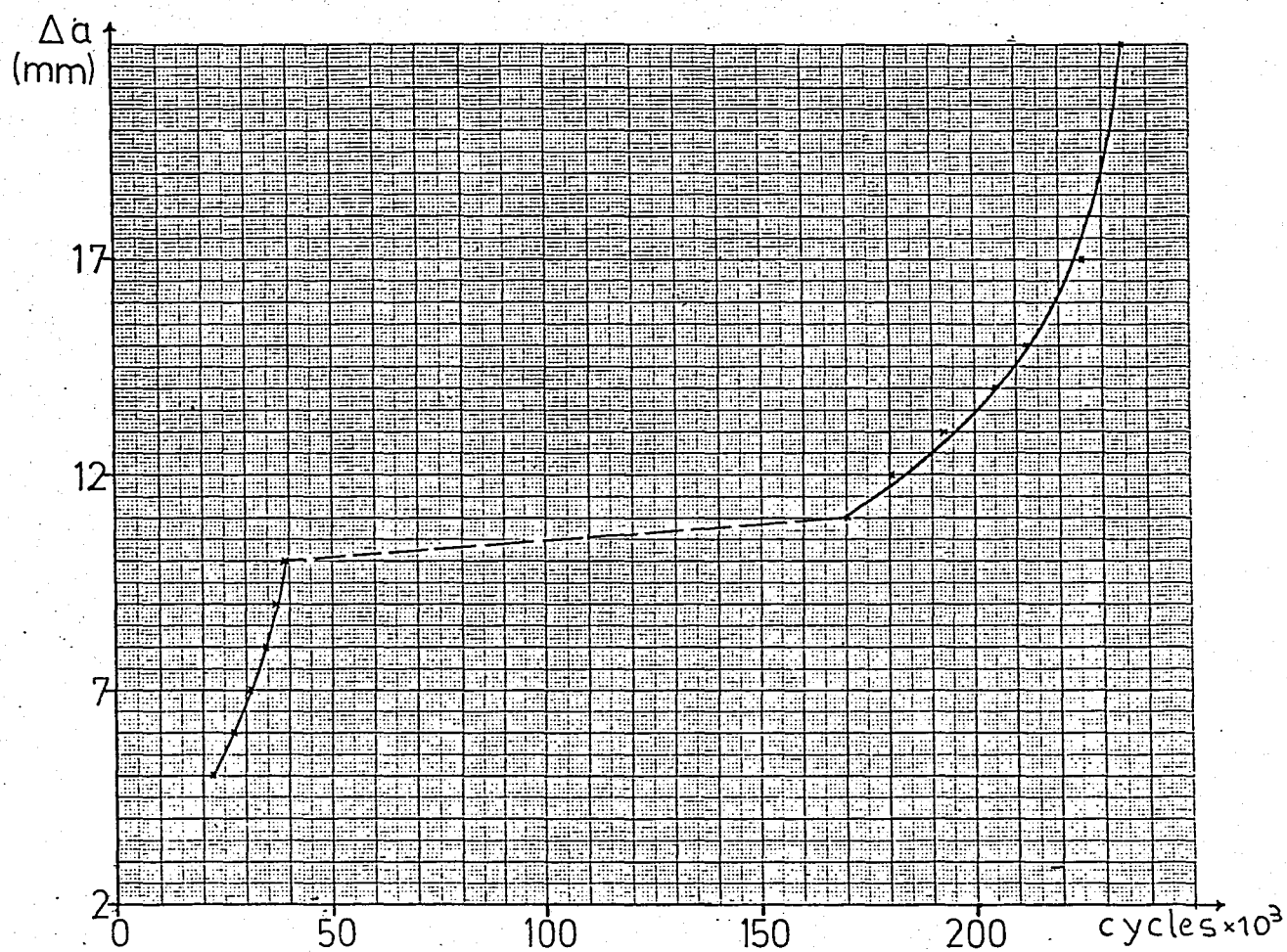


FIGURE 7.4- Fatigue behaviour of Specimen 18 (dotted zones indicate the crack retardation due to reduction in load)

APPENDIX D

(D-1)- Sample calculation for modulus of rupture for the bending test:

For rectangular cross section $I=bh^3/12$

$$b=h=9.55 \text{ mm}$$

$$I=(9.55^4)/12=693.3 \text{ mm}^4$$

$$\text{Simple flexure formula: } \sigma = Mc/I \quad (12)$$

$$c=h/2=4.75 \text{ mm}$$

For three point bending $M=PS/4$

where S:Span length

P:Applied load (maximum)

$$S=63.5 \text{ mm}$$

$$P=236 \text{ kg (for Specimen 115)}$$

$$\text{Using equation (12) yields } \sigma = 25.6 \text{ kg/mm}^2$$

REFERENCES

- 1- Liebowitz H., "FRACTURE" Vol III, Academic Press, New York (1971), pp. 646-673 .
- 2- Albrecht P., Andrews W.R., J.P. Gudas, J.A. Joke, Loss F.J. Mc.Cabe D.E., Schmidh D.W., Van Der Sluys W.A., "Tentative test procedure for determining the plane strain J_1 -R curve", Journal of testing and Evaluation, Vol 10, No 6, pp. 245-251 .
- 3- Frost N.E., Marsh K.J., Pook L.P., "Metal Fatigue", Clarendon press, Oxford (1974), pp. 203-222 .
- 4- Knott J.F., "Fundamentals of Fracture Mechanics", Butterworth group, London (1973), pp. 53-65, 105-112, 130-149, 164-174, 239-260 .
- 5- Davis H.E., Troxell G.E., Wiskocil C.T., "The Testing and Inspection of Engineering Materials", Mc Graw Hill, New York, (1961), pp. 116-122, 125-131, 165-178 .
- 6- Hertzberg R.W., "Deformation and Fracture Mechanics of Engineering Materials", John Wiley and Sons, New York, (1976), pp. 237, 255-271, 279-289, 293-297, 378-400, 466-495 .
- 7- Van Vlack H.L., "Elements of Materials Science and Engineering" Addison-Wesley Publishing Company, Massachusetts (1980) pp. 487-490 .
- 8- Rolfe T.S., Barsom M.J., "Fracture and Fatigue Control in Structures", Prentice Hall, New Jersey (1977), pp. 30-42, 55-77 232-236, 246-249, 292-304 .
- 9- Tetelman A.S., Mc Evily A.J., "Fracture of Structural Materials", John Wiley and Sons, New York (1967), pp. 38-56, 71-81, 348-367, 424-440 .
- 10- Fash J., Socie D.F., "Fatigue behaviour and mean effects in Gray Cast iron", International Journal of fatigue, July 1982, pp. 137-142 .
- 11- Brooksbank D., Andrews K.W., "Stress fields around inclusions and their relation to mechanical properties", Iron and Steel Institute Journal, Vol 210 (1972), pp. 246-250 .

- 12- Metals Handbook, American Society for Metals (1967)
Vol I, pp.349-366 .
- 13- B.F.Brown, "A new stress corrosion cracking test for high strength alloys", Materials Research and Standards, March 1966, pp.129 .
- 14- R.O.Ritchie, "Why ductile fracture mechanics", Journal of Engineering Materials and Technology, January 1983, pp.1-5
- 15- Landes, Walker, Clarke, "Evaluation of estimation procedures used in J- δ testing", ASTM STP 668 (1979) .